NASA TECHNICAL MEMORANDUM

NASA TM X-1665

NASA TM X-1665

EFFECT OF LARGE SIDESLIP ANGLES ON STABILITY CHARACTERISTICS OF A T-TAIL TRANSPORT CONFIGURATION

by Edward J. Ray

Langley Research Center

Langley Station, Hampton, Va.

NATIONAL AERONAUTICS AND SPACE ADMINISTRATION • WASHINGTON, D. C. • OCTOBER 1968

NASA TM X-1665

EFFECT OF LARGE SIDESLIP ANGLES ON STABILITY CHARACTERISTICS OF A T-TAIL TRANSPORT CONFIGURATION

By Edward J. Ray

Langley Research Center
Langley Station, Hampton, Va.

NATIONAL AERONAUTICS AND SPACE ADMINISTRATION

For sale by the Clearinghouse for Federal Scientific and Technical Information
Springfield, Virginia 22151 – CFSTI price $3.00

EFFECT OF LARGE SIDESLIP ANGLES ON STABILITY CHARACTERISTICS OF A T-TAIL TRANSPORT CONFIGURATION

By Edward J. Ray
Langley Research Center

SUMMARY

An investigation has been made to determine the effects of large sideslip angles on the static stability characteristics of a typical T-tail transport configuration. In addition, damping-in-roll derivatives were determined for the basic T-tail arrangement over an angle-of-attack range extending from about 0° to 36°. The effects of large sideslip variations on the pitching-moment characteristics were also ascertained for selected configurations. The study was made in the Langley high-speed 7- by 10-foot tunnel at a Mach number of 0.30 and a corresponding Reynolds number (based on mean aerodynamic chord) of 1.20×10^{6}.

The sideslip phase of this investigation was performed in two different manners. In the first method, the directional stability, lateral stability, and side-force parameters were determined by assuming linear variations of the static characteristics over a sideslip range of -5° to 5°. The complete configurations investigated in this manner exhibited positive effective dihedral and directional stability throughout an angle-of-attack range extending from about -4° to 22°. In order to assess this assumed linearity and to determine the lateral-directional characteristics over large sideslip ranges, several of the configurations were positioned at fixed angles of attack (range of 0° to 11°) and varied through sideslip angles extending from -22° to 22°. These tests indicated significant nonlinearities in the variation of yawing-moment coefficient with sideslip angle at relatively low angles of attack.

Two aft nacelle locations were investigated and it was determined from this limited study that the static directional stability characteristics could be substantially influenced at moderate angles of attack and sideslip by the position of the nacelles on the rearward portion of the fuselage. The horizontal T-tail exhibited a strong end-plate effect which generally resulted in favorable increments in the effective dihedral and directional stability of the configuration. Increases in sideslip angle resulted in increased nose-down pitching-moment contributions at angles of attack ranging from about 0° to 11°. The brief steady-state, forced-roll study indicated that the basic T-tail configuration would exhibit positive damping-in-roll characteristics at angles of attack ranging from 0° to 36° except at angles of attack near the wing stall angle.

INTRODUCTION

In recent years, there has been a trend toward designing commercial and business jet aircraft with aft-mounted engines and with horizontal stabilizers mounted high on the vertical tail. The combination of T-tail and aft engine offers several distinct advantages at normal operating angles of attack (see refs. 1 and 2); however, when integrating an aft-nacelle arrangement with high horizontal-tail position, careful consideration must be given to the stability characteristics at high angles of attack. The high tail must ultimately pass through an airplane wake system which could be augmented by the wake system of the aft-mounted nacelles, and once this occurs it is possible to encounter large losses in tail effectiveness. This concern stimulated a great deal of interest in the aerodynamic characteristics of T-tail configurations, and because of the scarcity of documented information for this type of aircraft, the National Aeronautics and Space Administration initiated a research program in 1964 to examine the stability and control characteristics of typical T-tail aircraft. (See refs. 3 to 8.) The initial studies were directed primarily toward the longitudinal stability characteristics.

The main purpose of the present wind-tunnel study was to determine the static lateral and directional stability characteristics of a typical T-tail transport arrangement at large angles of sideslip in the normal operating angle-of-attack range. The basic model of the present investigation was identical to the T-tail configuration discussed in references 3 to 5. Selected results which were determined for this "typical" T-tail arrangement have also been utilized in the analyses presented in references 2, 7, 8, and 9. In addition to the static sideslip results, pitching-moment and lift characteristics were determined for several of the configurations at a sideslip angle of zero through an angle-of-attack range varying from about -4° to 22°.

Pitching-moment characteristics through large sideslip ranges and the rate of change of rolling-moment coefficient with wing-tip helix angle were also determined for selected configurations. The investigation was conducted in the Langley high-speed 7- by 10-foot tunnel at a Mach number of 0.30 and a Reynolds number of 1.20×10^{6}, based on the wing mean aerodynamic chord.

SYMBOLS

The data presented in this paper are referred to the body-axis system with the exception of lift, which is referred to the stability-axis system. All the data contained in this paper are referred to a moment center located at the 0.40 point of the mean aerodynamic chord of the wing. (See fig. 1.) The coefficients were nondimensionalized by using the geometry of the basic wing. (See table I.)

The units used for the physical quantities in this report are given both in the U.S. Customary Units and in the International System of Units (SI). Factors relating the two systems are given in reference 10.

b reference wing span, 46.40 in. (117.86 cm)

$\bar{c}$ mean aerodynamic chord of wing, 6.69 in. (16.99 cm)

C_L lift coefficient, $\frac{\text{Lift}}{qS}$

C_l rolling-moment coefficient, $\frac{\text{Rolling moment}}{qSb}$

$(\Delta C_l)_H$ effective change in rolling-moment coefficient due to horizontal tail

$(\Delta C_l)_t$ effective change in rolling-moment coefficient due to combination of vertical and horizontal tails

C_{l_β} effective-dihedral parameter, $\frac{\partial C_l}{\partial \beta}$

C_{l_p} rate of change of rolling-moment coefficient with wing-tip helix angle $pb/2V$

C_m pitching-moment coefficient, $\frac{\text{Pitching moment}}{qS\bar{c}}$

C_n yawing-moment coefficient, $\frac{\text{Yawing moment}}{qSb}$

$(\Delta C_n)_H$ effective change in yawing-moment coefficient due to horizontal tail

$(\Delta C_n)_t$ effective change in yawing-moment coefficient due to combination of vertical and horizontal tails

C_{n_β} directional-stability parameter, $\frac{\partial C_n}{\partial \beta}$

C_Y side-force coefficient, $\frac{\text{Side force}}{qS}$

$(\Delta C_Y)_H$ effective change in side-force coefficient due to horizontal tail

$(\Delta C_Y)_t$ effective change in side-force coefficient due to combination of vertical and horizontal tails

C_{Y_β} side-force parameter, $\frac{\partial C_Y}{\partial \beta}$

p rate of roll, radians per unit time

q free-stream dynamic pressure, lb/ft^2 (N/m^2)

S area of wing, including body intercept, 1.92 ft^2 (0.1784 m^2)

V velocity

i_t incidence of horizontal tail (positive when trailing edge is down), degrees

α angle of attack, degrees

β sideslip angle, degrees

Model component designations:

F fuselage

W basic wing

W_f basic wing with fillets (see fig. 1)

V basic vertical tail

V_1 flat-plate vertical tail, leading edge swept forward

V_2 flat-plate vertical tail, leading edge swept back

H horizontal tail

N nacelle in basic location (leading edge at fuselage station 31.70 in. (80.52 cm))

N_{aft} nacelle in aft location (leading edge at fuselage station 35.71 in. (90.70 cm))

MODEL DESCRIPTION

The basic configuration of this investigation was identical to the basic model utilized in the wind-tunnel study described in reference 4. A drawing of the basic model is shown in figure 1 and geometric characteristics of the model components are presented in table I.

Fuselage

The typical cross section of the model fuselage had slightly flattened sides, a circular-arc bottom portion, and a larger circular-arc top portion. Except for small circular sections near the nose and the aft part of the fuselage, the fuselage was pear-shaped. (See fig. 1.)

Wing

The wing was composed of NACA 64A409 airfoil sections oriented in the streamwise direction. As shown in figure 1, the wing was affixed to the fuselage in a relatively low position. Several tests were conducted with the inboard portion of the wing trailing edge filled in with fillets. (See fig. 1.) The fillets were constructed of 0.125-in. (0.318-cm) flat-plate material with beveled trailing edges.

Horizontal and Vertical Tails

The horizontal and vertical tails were made up of NACA 0009 airfoil sections oriented streamwise. Provisions were made to deflect the entire horizontal tail for longitudinal control. In addition to the basic vertical tail, a flat-plate vertical tail, having an identical planform with rounded leading and trailing edges, was investigated with the leading edge swept both forward V_1 and back V_2. (See table I.) The centroid of area of the flat-plate vertical tail was positioned at fuselage station 45.00 in. (114.30 cm) in both sweep conditions.

Nacelles

Details of the basic nacelle arrangement are illustrated in figure 1. The nacelles were investigated in the location shown in figure 1 and in a more rearward location. In the rearward position, the nacelles were located $0.60\bar{c}$ (4.01 in. or 10.18 cm) aft of the basic position shown in figure 1 with the lip of the nacelles at fuselage station 35.71 in. (90.70 cm). In both of the nacelle positions the orientation of the nacelle center line with respect to the model reference planes remained constant.

TESTS AND CORRECTIONS

This experimental study was made in the Langley high-speed 7- by 10-foot tunnel with the slots in the test section closed. The average test conditions during the investigation were a free-stream Mach number of 0.30, a free-stream dynamic pressure of 124 lb/ft^2 (5937 N/m^2), and a Reynolds number based on $\bar{c}$ of 1.20×10^6.

The test models were sting mounted and the forces and moments were measured by means of a six-component strain-gage balance mounted within the fuselage. (Only five components of data have been presented herein. Drag results have been excluded from this stability analysis since the drag characteristics for these configurations were presented in detail in ref. 4.) The angles of attack and sideslip have been corrected for combined deflection of the sting-support system and balance under load. Jet-boundary corrections calculated by the method of reference 11 have been applied to the angle-of-attack values. Blockage corrections determined by the method of reference 12 were utilized in the reduction of the data.

The sideslip results of this study were obtained by utilizing two different test techniques. In the first of these methods, the various test configurations were affixed at a sideslip angle and then displaced through an angle-of-attack range which extended from about -4° to 22°. The sideslip angles investigated were 5°, 0°, and -5°. In this method, the sideslip parameters C_{l_β}, C_{n_β}, and C_{Y_β} which are included in figures 2 to 8 were derived by assuming that the model sideslip characteristics were linear over the sideslip range of -5° to 5°. Since the primary purpose of this investigation was to determine the static lateral-directional characteristics of the T-tail arrangement at large sideslip angles, and since there was concern regarding the linearity of the sideslip variations, data were also obtained by placing the test configurations at a fixed angle of attack (0.2°, 5.6°, and 11.0°) and displacing the test configurations through sideslip ranges extending from about -22° to 6° and/or -6° to 22°. The data which were obtained in this manner are shown in figure 9.

The steady-state forced-roll technique used to determine the change in the rolling-moment coefficient with wing-tip helix angle C_{l_p} is described thoroughly in reference 13. Because of the length of the fuselage, it was necessary to position the model center of mass well ahead of the center of rotation of the forced-roll test equipment. Tests which were conducted with different longitudinal locations of the model, as well as theoretical estimates, indicated that the roll results could be corrected satisfactorily for this "offset" position, but the corrected yaw and side-force parameters were inconsistent and appeared to be questionable. The yaw and side-force derivatives C_{n_p} and C_{Y_p}, therefore, have been omitted from the results in this paper.

PRESENTATION OF RESULTS

The data which were determined in this wind-tunnel investigation are presented in the following figures. The configuration code is defined in the section entitled "Symbols."

DISCUSSION

Static Aerodynamic Characteristics at Small Sideslip Angles

As mentioned previously, the sideslip parameters shown in figures 2 to 8 were obtained by assuming a linear variation of the lateral-directional and side-force characteristics over a range of sideslip angle β from -5° to 5°. The longitudinal data (C_L and C_m) included in figures 2 to 8 were determined at a sideslip angle of 0°. The drag characteristics of the configurations discussed herein are presented in reference 4.

It will be noted from figure 2(b) that the wing has a favorable effect on the directional-stability parameter C_{n_β} up to an angle of attack of about 8°, which corresponds to the angle-of-attack range at which the lift-curve slope (fig. 2(a)) begins to diminish. Addition of the vertical tail (fig. 2(b)) resulted in large positive increments in the directional-stability parameter C_{n_β} and an increase in the effective-dihedral characteristics, as indicated by the negative increment in C_{l_β}. It should be noted here that the assumed center-of-gravity position at $0.40\bar{c}$ is probably comparable to the most rearward position that would be experienced by a typical T-tail transport aircraft. The placement of the horizontal tail at the tip of the sweptback fin causes a sizable increase in the static directional stability level (fig. 3(b)), which is presumed to be due to an end-plate effect.

The sideslip-parameter results in figure 5(b) indicate that the complete basic configuration exhibits positive effective dihedral (indicated by negative values of C_{l_β}) and static directional stability throughout the test angle-of-attack range. It will be noted that at the wing stall angle of about 12° (see fig. 5(a)) there is a marked decrease in the effective-dihedral parameter and an increase in the directional-stability parameter.

The results of reference 4 have indicated that the longitudinal positioning of the nacelles on the rearward portion of the fuselage has very important effects on the pitching-moment characteristics of T-tail aircraft at high angles of attack. At the lower angles of attack, it will be noted from figure 7(a) that the rearward movement of the nacelle and nacelle pylon area results in an expected increase in the longitudinal stability level. A review of the lateral-directional characteristics (fig. 7(b)) indicates that the addition of the nacelles in the basic position results in a sizable reduction in the static directional stability at low angles of attack, whereas the more rearward nacelles had very little effect below an angle of attack of 7°. The change in directional stability exhibited with the nacelles located in the basic position is probably associated with a reduction in the favorable, direct, and wing-sidewash effects at low to moderate angles of attack. (Note C_{n_β} and C_{Y_β} variations for F, FW, FWV in fig. 2(b), and FV in fig. 3(b).) Figure 7(b) indicates that at angles of attack above 8°, both nacelle arrangements favorably affected the static directional stability characteristics of the configuration. Figure 8(b) illustrates that deflection of the horizontal tail apparently produced favorable flow gradients on the vertical tail and resulted in a sizable increase in the static directional-stability parameter with insignificant changes in the effective-dihedral parameter.

Static Stability Characteristics Through Large Sideslip Ranges

As mentioned previously, tests were performed over large ranges of sideslip angle to ascertain the effects on the static stability behavior of the T-tail arrangements and to evaluate the linearity in the variations of the stability characteristics. A comparison of the $\partial C_l/\partial\beta$ and $\partial C_n/\partial\beta$ slopes in figure 9(a) with the C_{l_β} and C_{n_β} values for the FW arrangement in figure 2(b) at an angle of attack of 11° suggests that there is good agreement in the results obtained by the two methods of testing for linear situations (linear variation of moment and force coefficients with β). In reviewing the results shown in figure 9, however, it will be noted that significant nonlinearities occur, particularly in the yawing-moment coefficients, for the configurations with vertical tail on at an angle of attack of 11° in the relatively low sideslip-angle range. The reversal in the slope of the C_n variation with β occurring at sideslip angles from about 4° to 8° for these configurations is probably due to adverse wake effects on the vertical tail and, in addition, a possible reduction in the favorable horizontal-tail end-plate effect. (Compare figs. 9(e) and 9(b).)

In addition, the results in figure 9 indicate pronounced nonlinear variations in the lateral, directional, and side-force characteristics at the higher angles of sideslip, that is, at β of 8° and above. The most significant nonlinearities are exhibited for the configurations with vertical tail on at the highest angle of attack (for instance, see fig. 9(b)); however, sizable nonlinearities are evident for the configurations without the vertical tail and in the results obtained at the lower angles of attack. As in the low β range, the sideslip characteristics in the higher range of β suggest that these nonlinearities are primarily associated with the wake effects on the vertical tail. The nonlinear "tail-off" trends at the higher angles of sideslip imply that the lateral, directional, and side-force characteristics are also affected, to a lesser degree, by either sidewash effects on the rearward portion of the fuselage or changes in the cross-flow characteristics around the wing-body combination.

The results in reference 14 indicate that sizable increases in nose-down pitching-moment increments can be experienced with increases in sideslip angle for this type of low-wing configuration as a result of the cross-flow characteristics over the wing and around the fuselage. The pitching-moment results shown in figure 10(a) for the configuration without nacelles illustrate this effect. Substantial increases in the nose-down pitching-moment coefficient are exhibited with increasing negative or positive sideslip angle. A comparison of the curves for angles of attack of 0.2° and 11.0° indicates that there is a reduction of this effect with increasing angle of attack. In addition, the results presented in reference 14 indicate that the variation of nose-down pitching-moment increments with sideslip can be affected by the position of the horizontal tail. In the case of the high T-tail, the results shown in reference 14 show that the nose-down pitching-moment effect should be augmented by the addition of the horizontal tail. A comparison of figures 10(b) and 10(c) illustrates that the addition of the T-tail results in sizable increases in the nose-down moment increment, particularly at the higher angles of sideslip. The results in figures 10(a) and 10(b) indicate that the nacelles also affect the variation of pitching-moment coefficient with sideslip angle. The addition of the nacelles to the rearward portion of the fuselage reduces the change in pitching-moment coefficients resulting from variations in sideslip angle.

The changes in sideslip characteristics resulting from the addition of the vertical and horizontal tails to several of the test configurations are shown in summary figures 11 to 13. The data in figure 11 indicate that the addition of the combination of vertical and horizontal tails favorably affected the static rolling- and yawing-moment characteristics of the nacelles-off configuration throughout the angle-of-attack and sideslip ranges of the study. The addition of the horizontal tail to the configuration with the aft nacelles (fig. 12) resulted in an increasing stabilizing trend of the rolling moment up to an angle of sideslip of about 12°. The end-plate effect of the horizontal tail resulted in increased static directional stability at the lower angles of attack and sideslip. A comparison of the data in figures 11 and 13 reveals that addition of nacelles in the aft location had very little effect on the static lateral-directional stability characteristics of this particular T-tail arrangement at angles of attack up to 11°. It is suspected, however, that at the higher angles of attack (where the aircraft wake system is more fully developed) the placement of nacelles on the rearward portion of the fuselage could have a substantial influence on the directional stability characteristics of the configuration.

Damping-in-Roll Characteristics of Basic Configuration

The results shown in figure 14 illustrate the damping-in-roll derivatives C_{l_p} that were determined experimentally and analytically for the basic T-tail configuration at angles of attack up to about 36°. There was good agreement between the experimental data and the values estimated by the method suggested in reference 13. In the lower angle-of-attack range, the damping in roll decreased (negative values of C_{l_p} indicate positive damping) with increasing angle of attack and became 0 at an angle of attack of about 12°, which corresponds to the approximate wing stall angle of the configuration. (See fig. 5(a).) The increase in positive damping in roll after an angle of attack of about 17° is directly related to the increase in the lift-curve slope at angles of attack of about 18°. (See fig. 5(a).)

CONCLUDING REMARKS

The present investigation was conducted in the Langley high-speed 7- by 10-foot tunnel at a Mach number of 0.30 and a corresponding Reynolds number (based on mean aerodynamic chord) of 1.20×10^6.

The investigation indicated that if linear variations of the lateral-directional derivatives were assumed over the sideslip range of -5° to 5° the basic T-tail configuration would exhibit positive effective dihedral and directional stability throughout an angle-of-attack range extending from about -4° to 22°. A detailed assessment of the lateral-directional characteristics, however, performed over large sideslip ranges indicated significant nonlinearities in the variation of yawing-moment coefficient with sideslip angle at relatively low angles of attack.

Two aft nacelle locations were investigated and it was determined from this limited study that the static directional stability characteristics could be substantially influenced at moderate angles of attack and sideslip by the position of the nacelles on the rearward portion of the fuselage. The horizontal T-tail exhibited a strong end-plate effect which generally resulted in favorable increments in the effective dihedral and directional stability of the configuration. Increases in sideslip angle resulted in increased nose-down pitching-moment contributions at angles of attack ranging from about 0° to 11°. The brief steady-state, forced-roll study indicated that the basic T-tail configuration would exhibit positive damping-in-roll characteristics at angles of attack ranging from 0° to 36° except at angles of attack near the wing stall angle.

Langley Research Center,
National Aeronautics and Space Administration,
Langley Station, Hampton, Va., July 23, 1968,
720-01-00-03-23.

REFERENCES

1. Multhopp, Hans: The Case for T-Tails. Aero Digest, vol. 70, no. 5, May 1955, pp. 32-35.

2. Polhamus, Edward C.: The Deep-Stall Problem of T-Tail Aircraft. Space/Aeronaut., vol. 45, no. 5, May 1966, pp. 106-108.

3. Taylor, Robert T.; and Ray, Edward J.: Deep-Stall Aerodynamic Characteristics of T-Tail Aircraft. Conference on Aircraft Operating Problems, NASA SP-83, 1965, pp. 113-121.

4. Ray, Edward J.; and Taylor, Robert T.: Effect of Configuration Variables on the Subsonic Longitudinal Stability Characteristic of a High-Tail Transport Configuration. NASA TM X-1165, 1965.

5. Ray, Edward J.; Lockwood, Vernard E.; and Henderson, William P.: Some Configuration Effects on Static Stability of Airplanes at High Angles of Attack and Low Speeds. Conference on Aircraft Aerodynamics. NASA SP-124, 1966, pp. 61-74.

6. White, Maurice D.; and Cooper, George E.: Simulator Studies of the Deep Stall. Conference on Aircraft Operating Problems, NASA SP-83, 1965, pp. 101-111.

7. Lina, Lindsay J.; and Moul, Martin T.: A Simulator Study of T-Tail Aircraft in Deep Stall Conditions. AIAA Paper No. 65-781, 1965.

8. Montgomery, Raymond C.; and Moul, Martin T.: Analysis of Deep-Stall Characteristics of T-Tailed Aircraft Configurations and Some Recovery Procedures. J. Aircraft, vol. 3, no. 6, Nov.-Dec. 1966, pp. 562-566.

9. Byrnes, A. L.; Hensleigh, W. E.; and Tolve, L. A.: Effect of Horizontal Stabilizer Vertical Location on the Design of Large Transport Aircraft. J. Aircraft, vol. 3, no. 2, Mar.-Apr. 1966, pp. 97-104.

10. Mechtly, E. A.: The International System of Units – Physical Constants and Conversion Factors. NASA SP-7012, 1964.

11. Gillis, Clarence L.; Polhamus, Edward C.; and Gray, Joseph L., Jr.: Charts for Determining Jet-Boundary Corrections for Complete Models in 7- by 10-Foot Closed Rectangular Wind Tunnels. NACA WR L-123, 1945. (Formerly NACA ARR L5G31.)

12. Herriot, John G.: Blockage Corrections for Three-Dimensional-Flow Closed-Throat Wind Tunnels, With Consideration of the Effect of Compressibility. NACA Rep. 995, 1950. (Supersedes NACA RM A7B28.)

13. Hayes, William C., Jr.; Kemp, William B., Jr.; and Thompson, Wilson E.: Wind-Tunnel Measurements and Estimated Values of the Rolling Stability Derivatives of a Variable-Sweep Airplane Configuration at Subsonic and Transonic Speeds. NASA TM X-600, 1961.

14. Polhamus, Edward C.: Some Factors Affecting the Variation of Pitching Moment With Sideslip of Aircraft Configurations. NACA TN 4016, 1958. (Supersedes NACA RM L55E20b.)

TABLE I.- GEOMETRIC CHARACTERISTICS OF MODEL COMPONENTS

Fuselage:	
Length	49.50 in. (125.73 cm)
Maximum width	5.80 in. (14.73 cm)
Maximum height	6.50 in. (16.51 cm)
Wing:	
Leading-edge sweep	28°
Span	46.40 in. (117.86 cm)
Root chord	9.50 in. (24.13 cm)
Tip chord	2.40 in. (6.10 cm)
Mean aerodynamic chord	6.69 in. (16.99 cm)
Area	1.92 ft^2 (0.1784 m^2)
Aspect ratio	7.8
Airfoil section	NACA 64A409
Horizontal tail:	
Leading-edge sweep	38°
Span	16.12 in. (40.95 cm)
Root chord	5.82 in. (14.78 cm)
Tip chord	1.67 in. (4.24 cm)
Mean aerodynamic chord	4.13 in. (10.49 cm)
Area	0.42 ft^2 (0.0390 m^2)
Aspect ratio	4.3
Taper ratio	0.29
Ratio of horizontal tail area to wing reference area	0.22
Airfoil section	NACA 0009
Vertical tail (basic):	
Leading-edge sweep	38°
Area	0.36 ft^2 (0.0334 m^2)
Airfoil section	NACA 0009
Vertical tail (flat plate):	
Leading-edge sweep	38° or -38°
Area	0.36 ft^2 (0.0334 m^2)
Airfoil section	flat plate 0.375 in. (0.953 cm) thick with rounded edges
Nacelle:	
Length	9.15 in. (23.24 cm)
Maximum diameter	2.30 in. (5.84 cm)
Inlet diameter	1.50 in. (3.81 cm)
Exit diameter	1.50 in. (3.81 cm)

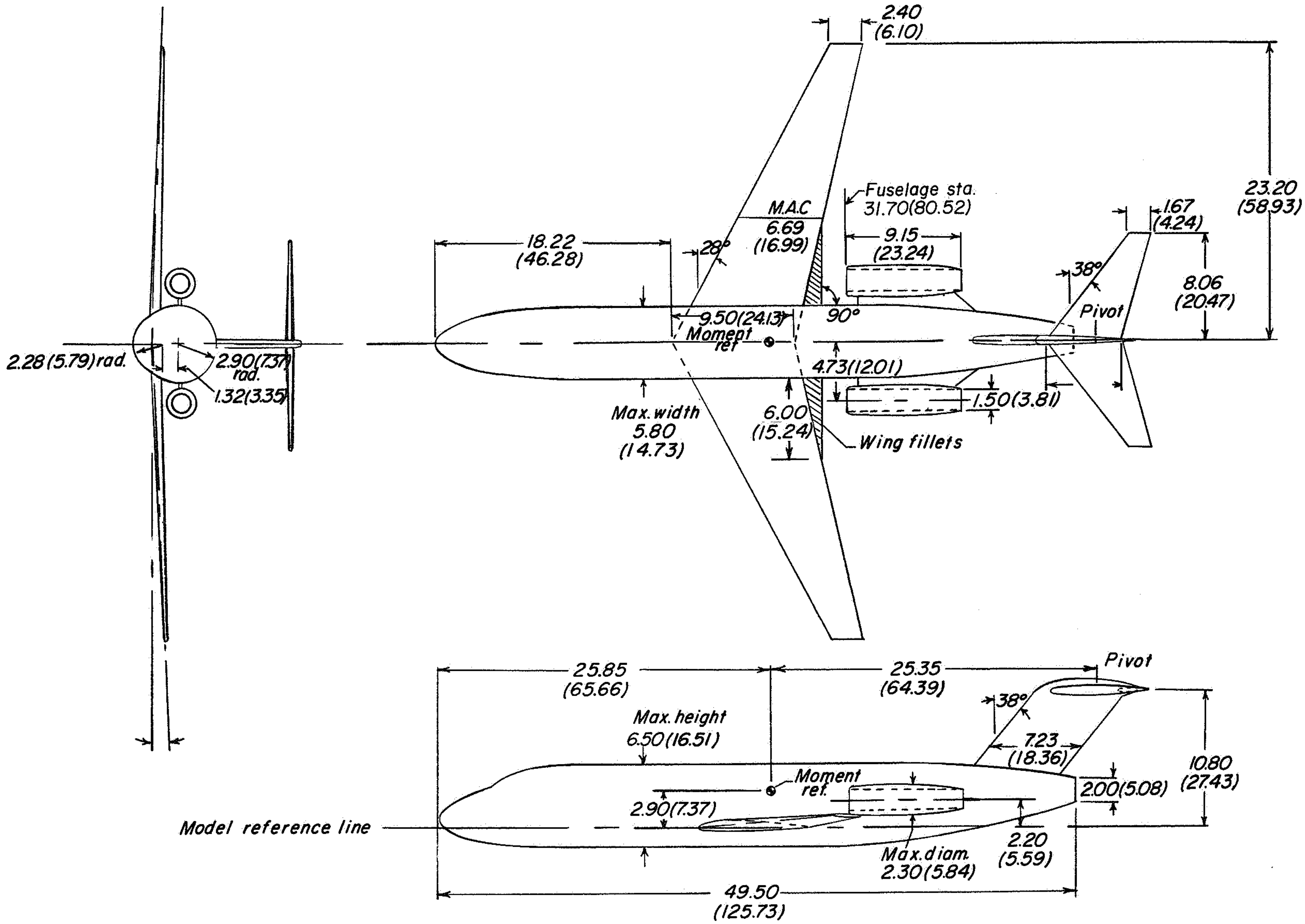

Figure 1.- Three-view drawing of basic configuration FWVHN. All linear dimensions are in inches (cm).

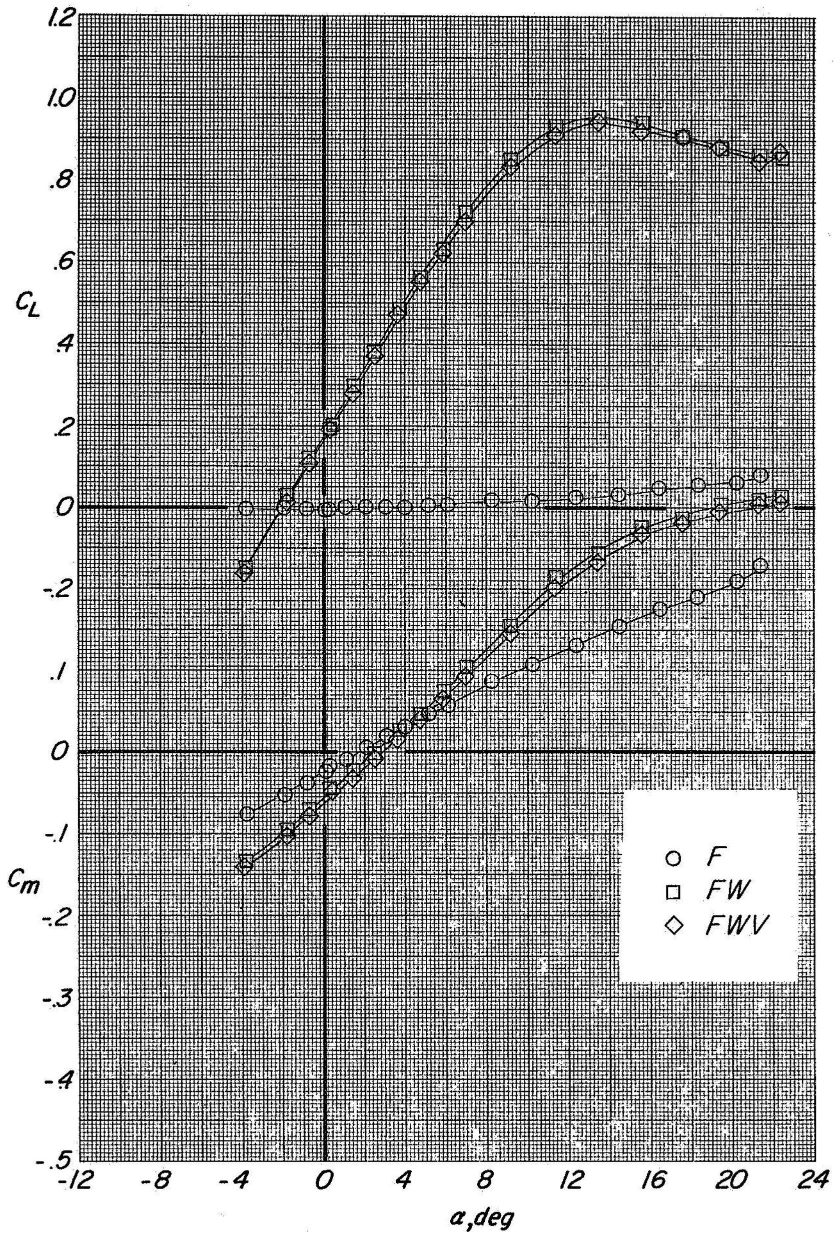

(a) Variation of C_L and C_m with α. $\beta = 0^{o}$.

Figure 2.- Lift, pitch, lateral, directional, and side-force characteristics of F, FW, and FWV.

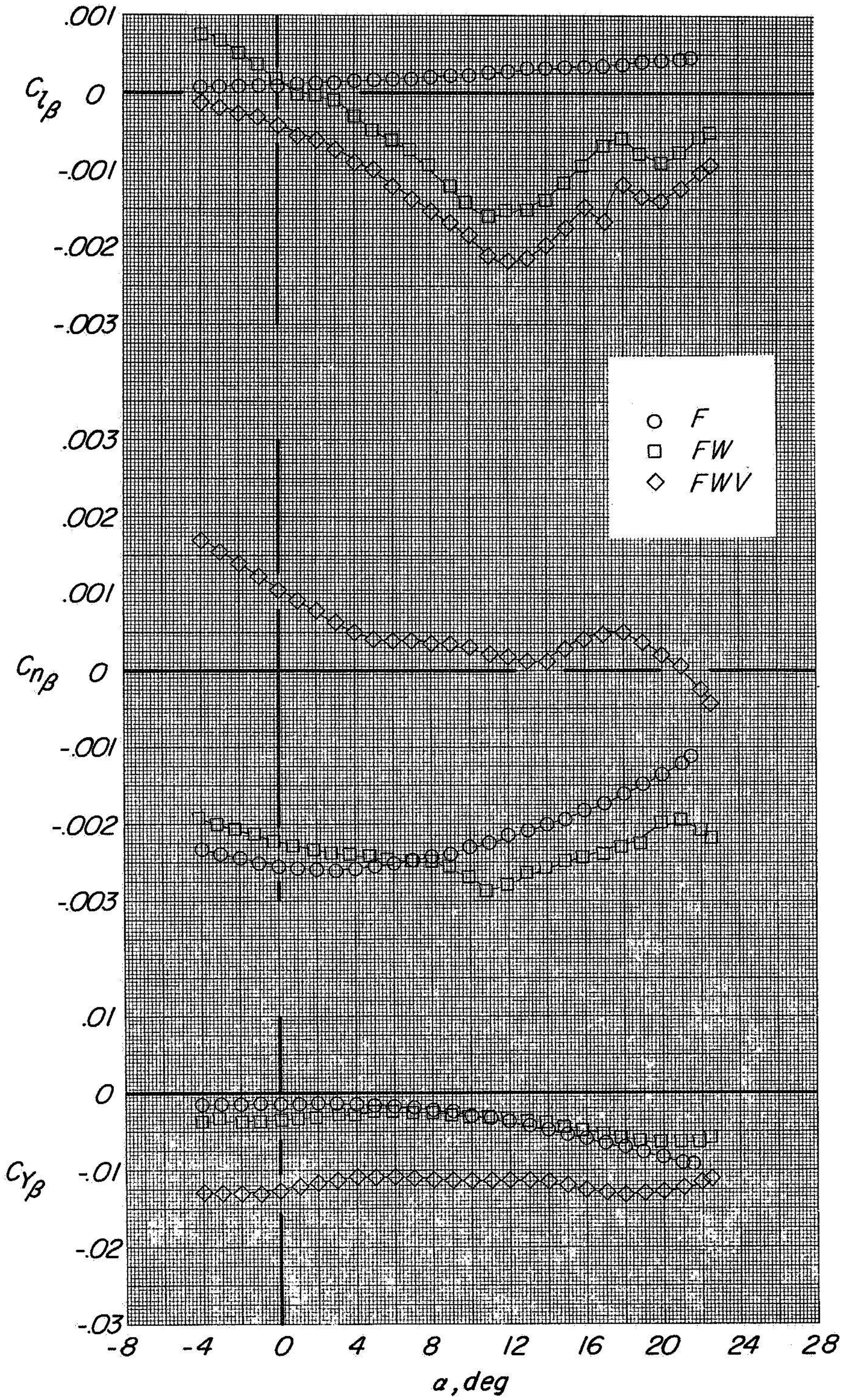

(b) Variation of C_{l_β}, C_{n_β}, and C_{Y_β} with α.

Figure 2.- Concluded.

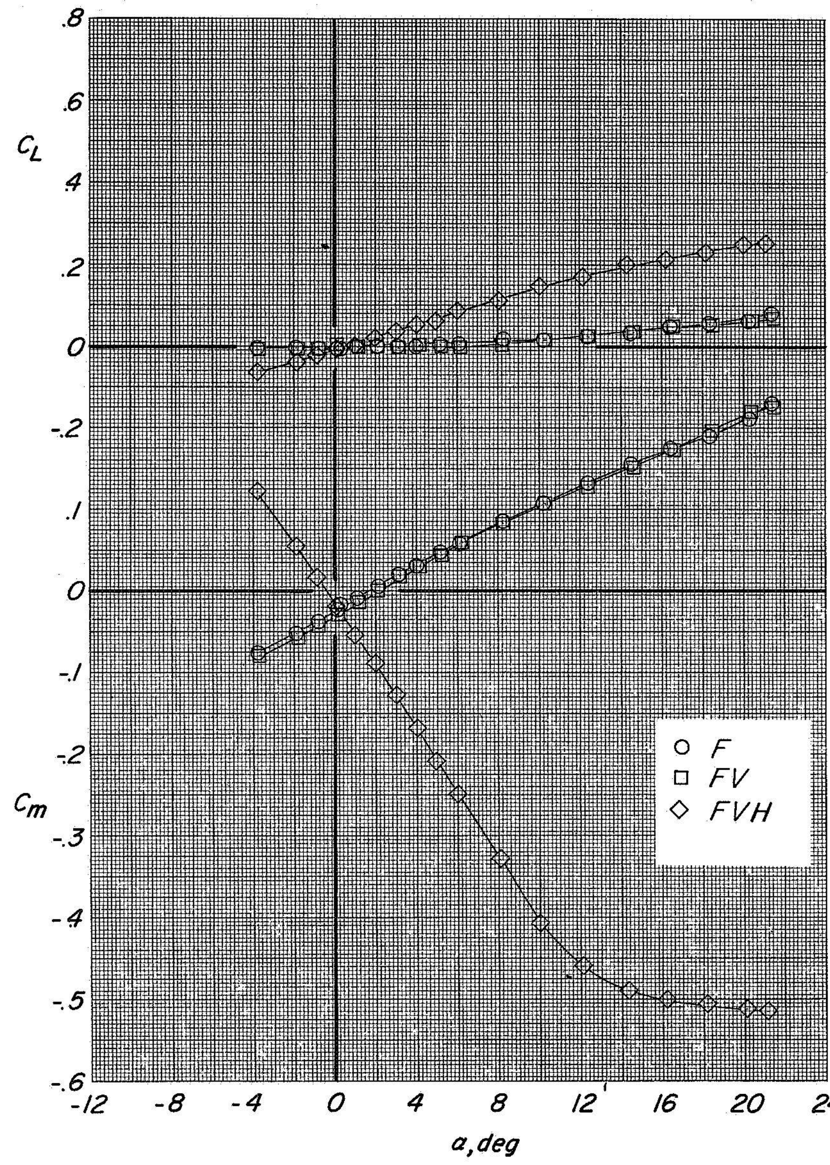

(a) Variation of C_L and C_m with α. $\beta = 0^0$.

Figure 3.- Lift, pitch, lateral, directional, and side-force characteristics of F, FV, and FVH. $\left(i_t \approx 0^0.\right)$

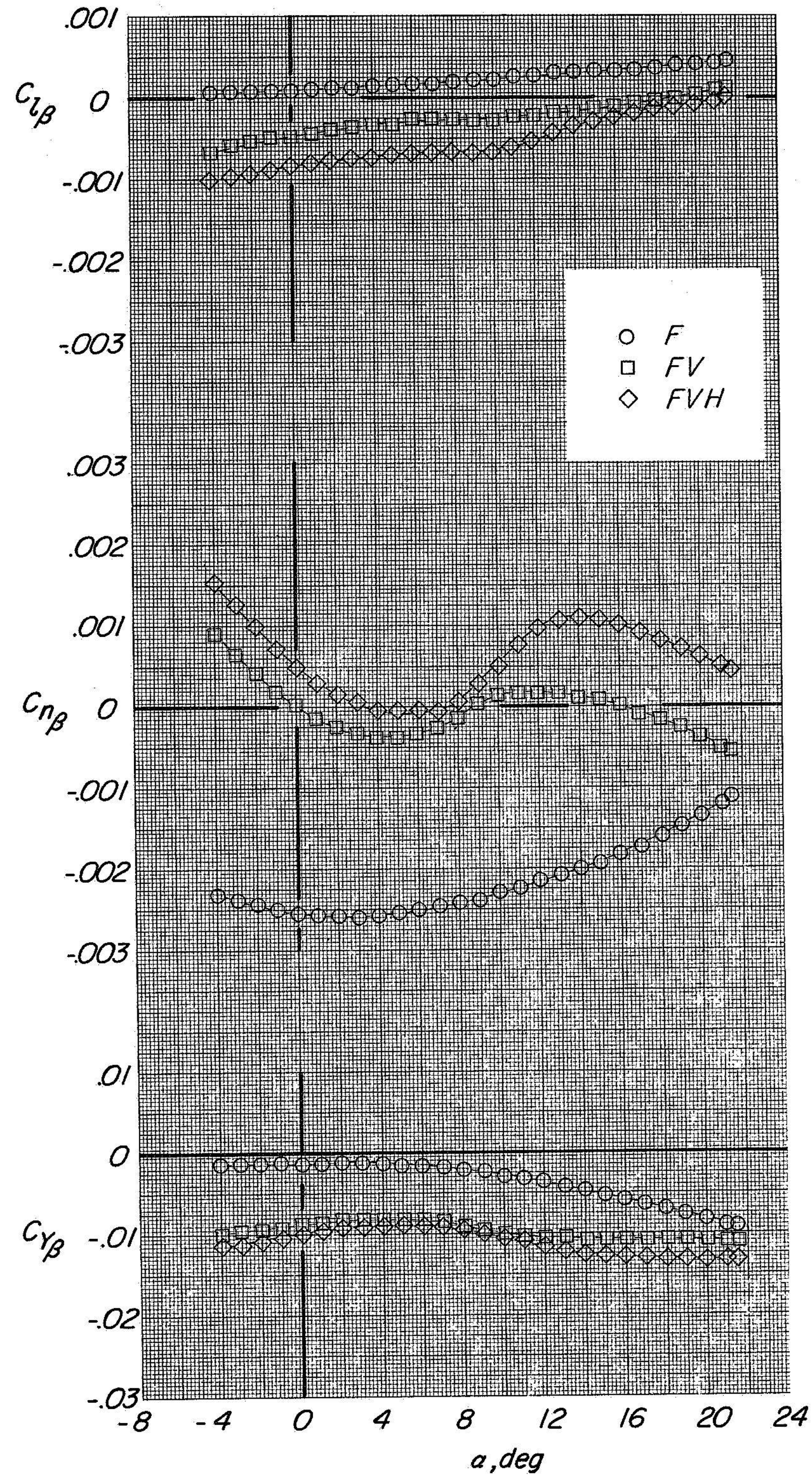

(b) Variation of C_{l_β}, C_{n_β}, and C_{Y_β} with α.

Figure 3.- Concluded.

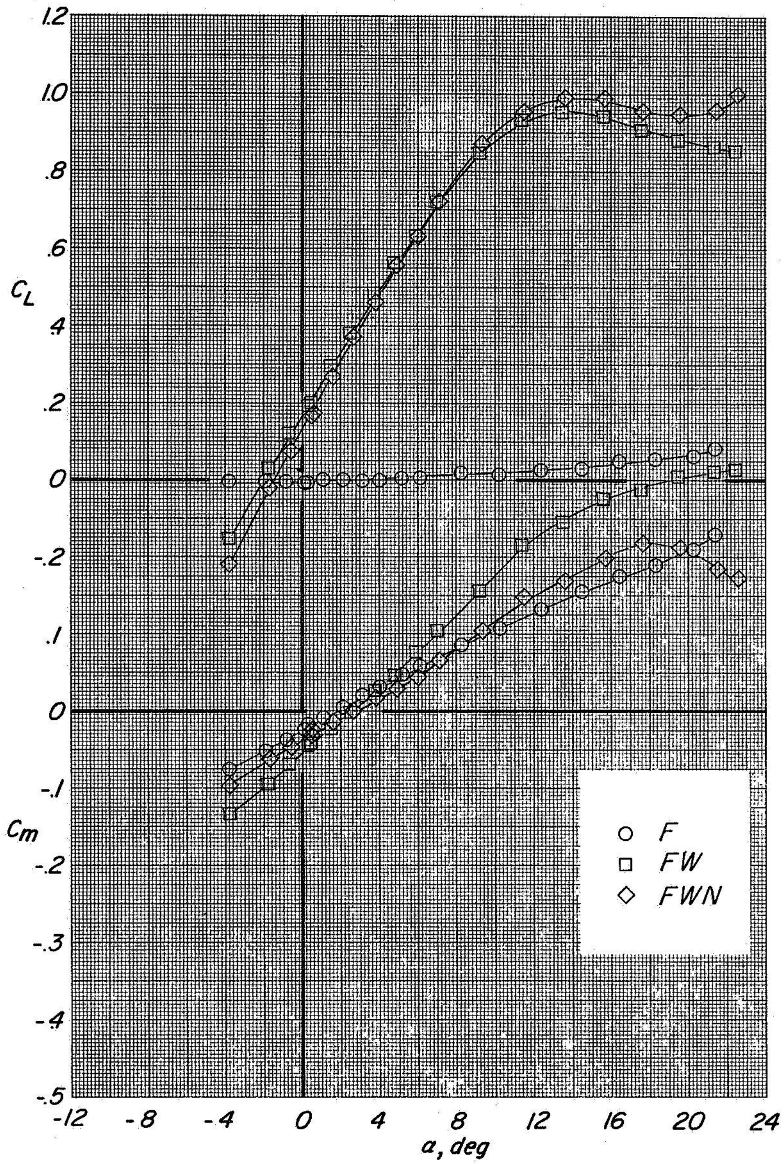

(a) Variation of C_L and C_m with α. $\beta = 0^0$.

Figure 4.- Lift, pitch, lateral, directional, and side-force characteristics of F, FW, and FWN.

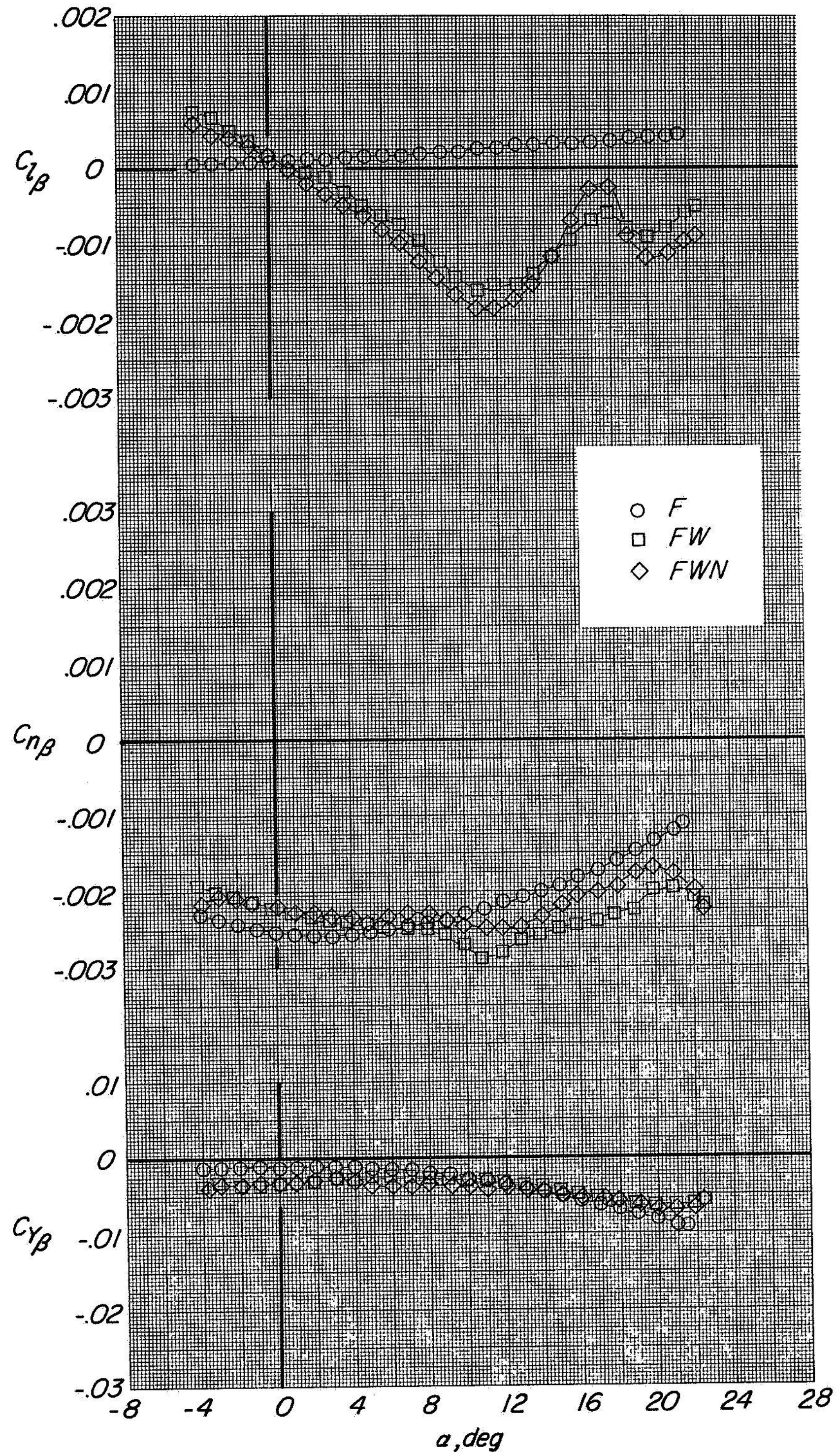

(b) Variation of C_{l_β}, C_{n_β}, and C_{Y_β} with α.

Figure 4.- Concluded.

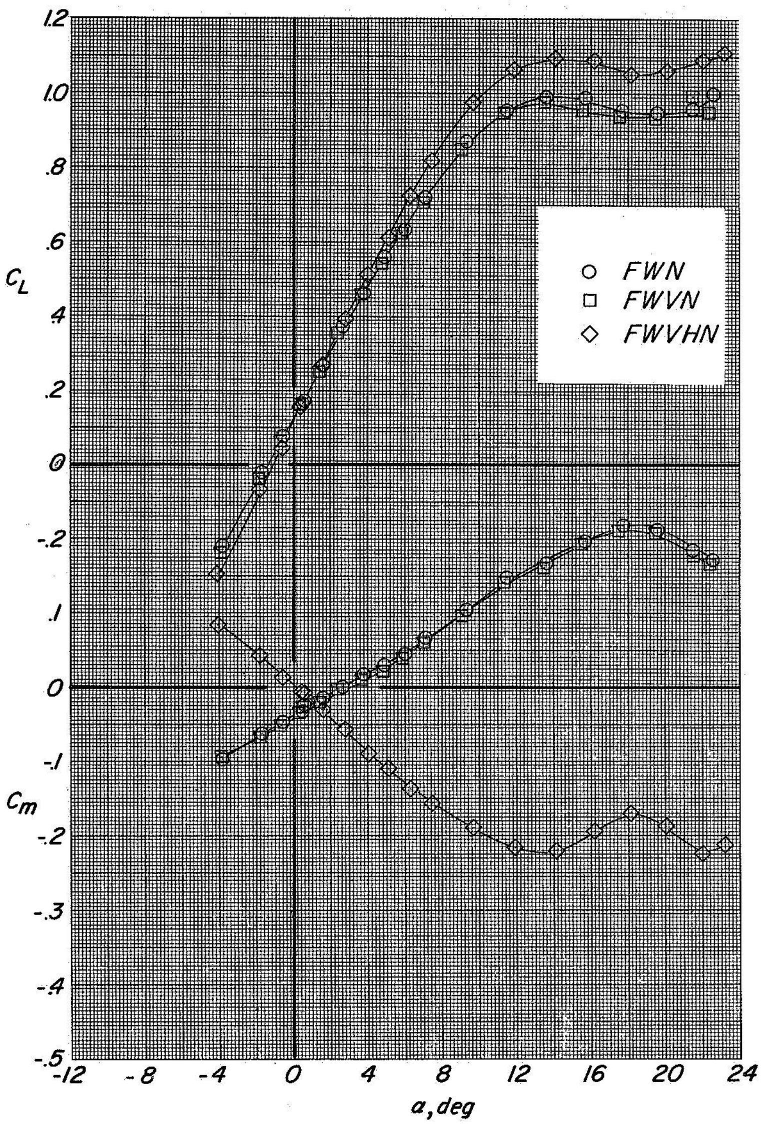

(a) Variation of C_L and C_m with α. $\beta = 0^{\circ}$.

Figure 5.- Lift, pitch, lateral, directional, and side-force characteristics of FWN, FWVN, and FWVHN. $\left(i_t \approx -0.5^{\circ}.\right)$

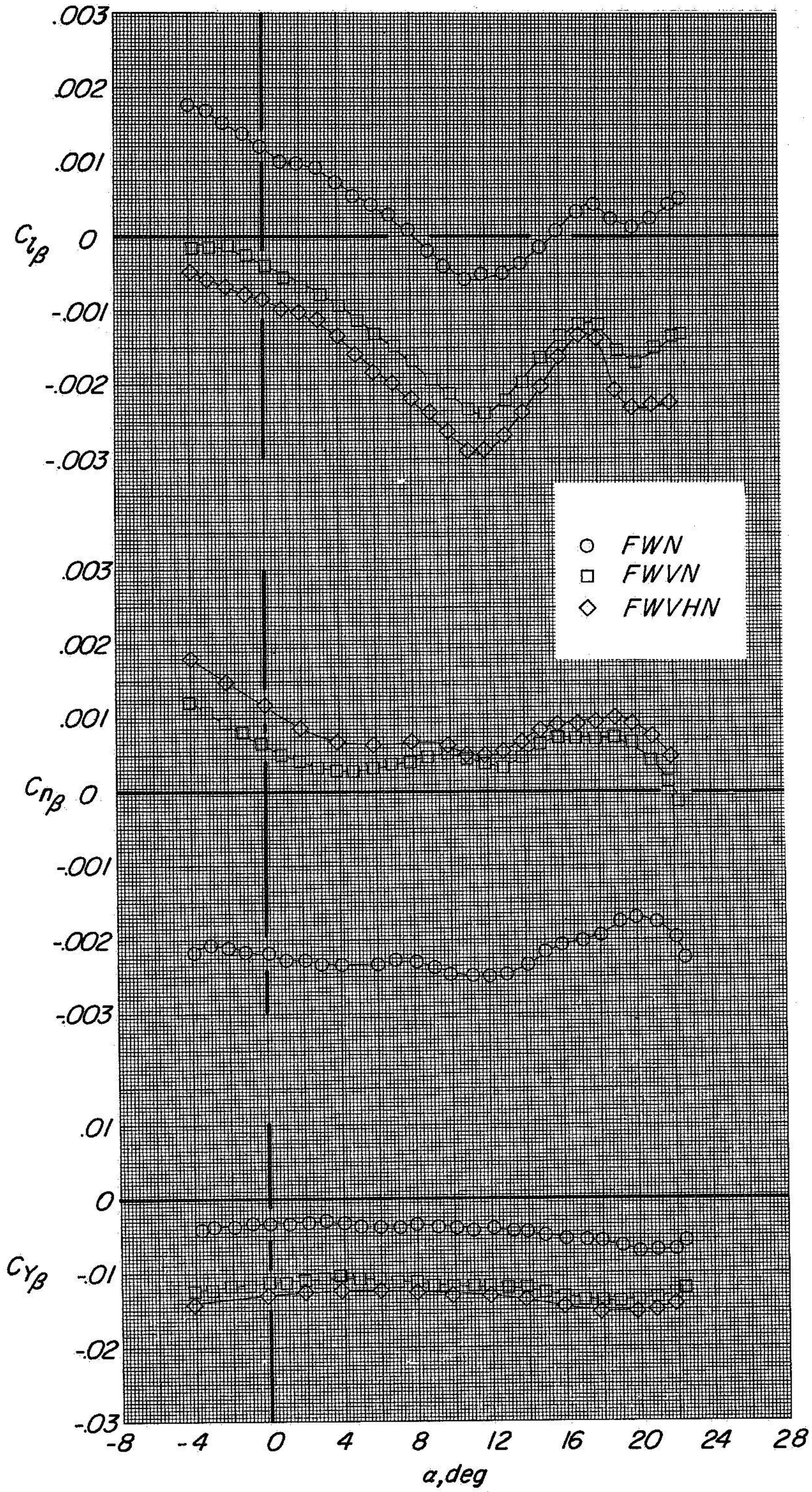

(b) Variation of C_{l_β}, C_{n_β}, and C_{Y_β} with α.

Figure 5.- Concluded.

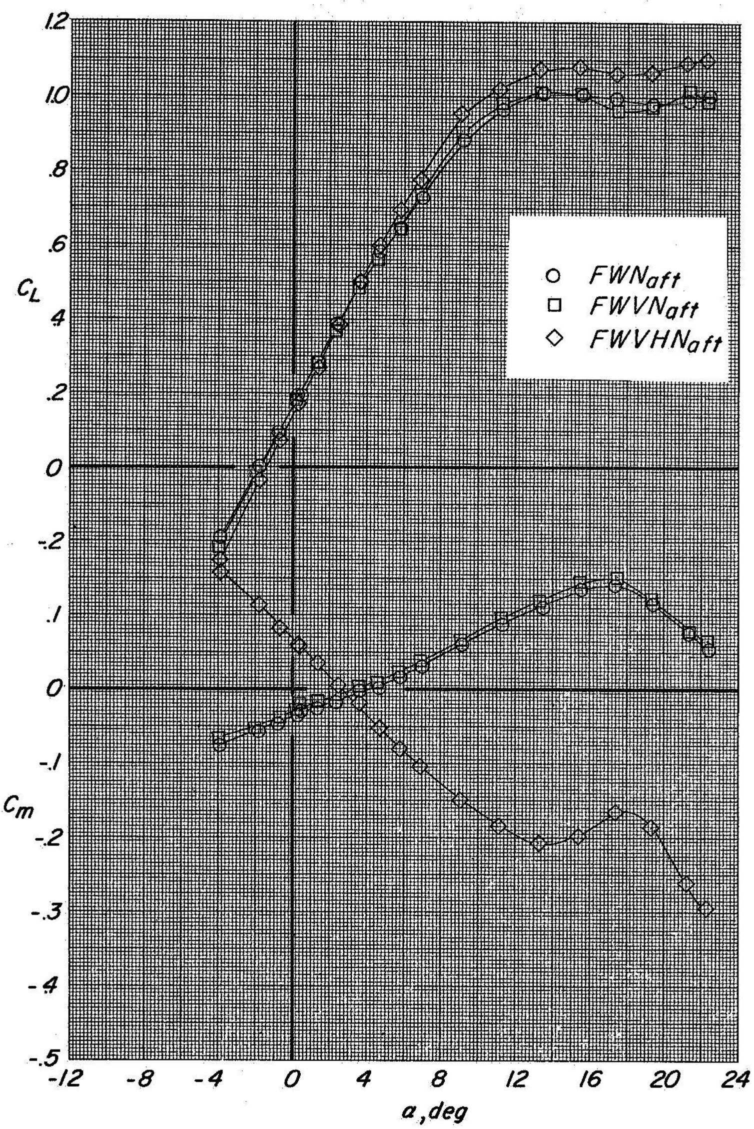

(a) Variation of C_L and C_m with α. $\beta = 0^o$.

Figure 6.- Lift, pitch, lateral, directional, and side-force characteristics of FWN_{aft}, $FWVN_{aft}$, and $FWVHN_{aft}$. $\left(i_t \approx -1.5^o.\right)$

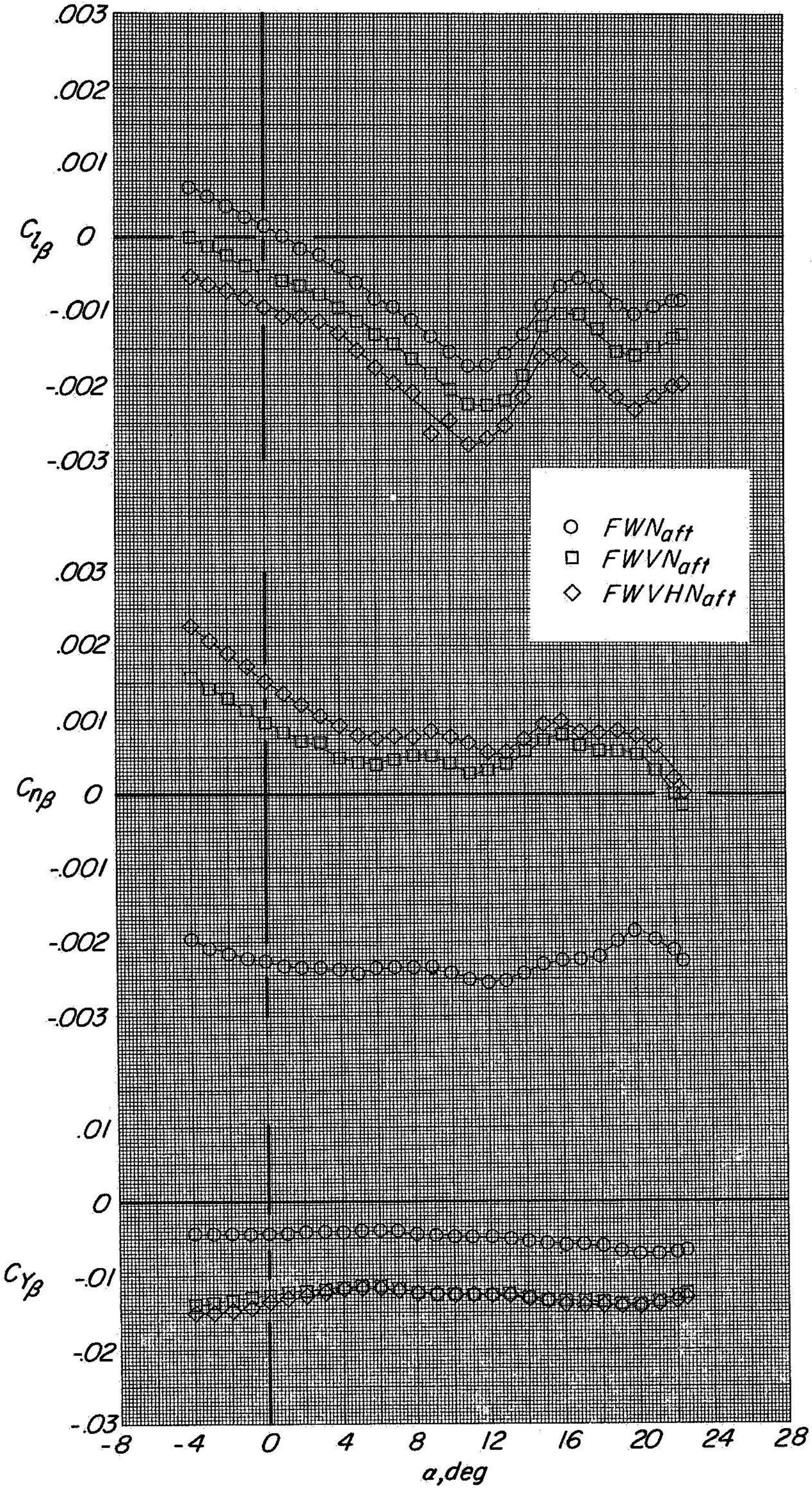

(b) Variation of C_{l_β}, C_{n_β}, and C_{Y_β} with α.

Figure 6.- Concluded.

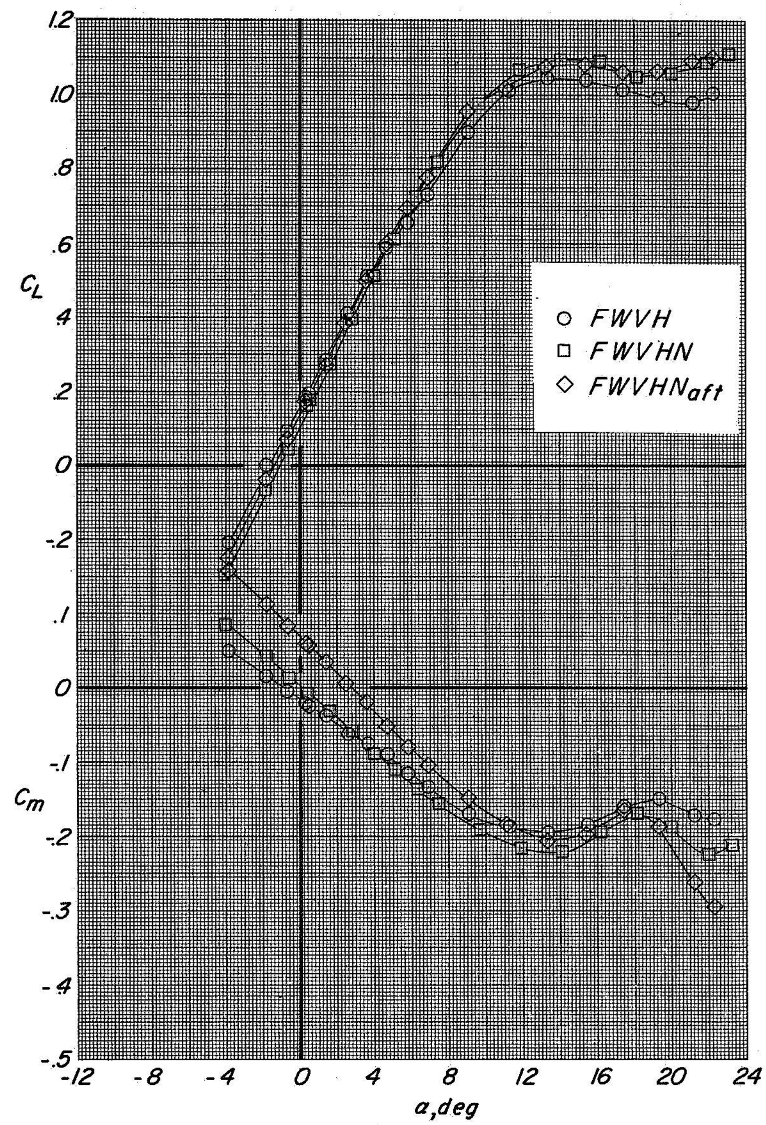

(a) Variation of C_L and C_m with α. β = 0°.

Figure 7.- Lift, pitch, lateral, directional, and side-force characteristics of FWVH ($i_t \approx -0.5^\circ$), FWVHN ($i_t \approx -0.5^\circ$), and FWVHN$_{aft}$ ($i_t \approx -1.5^\circ$).

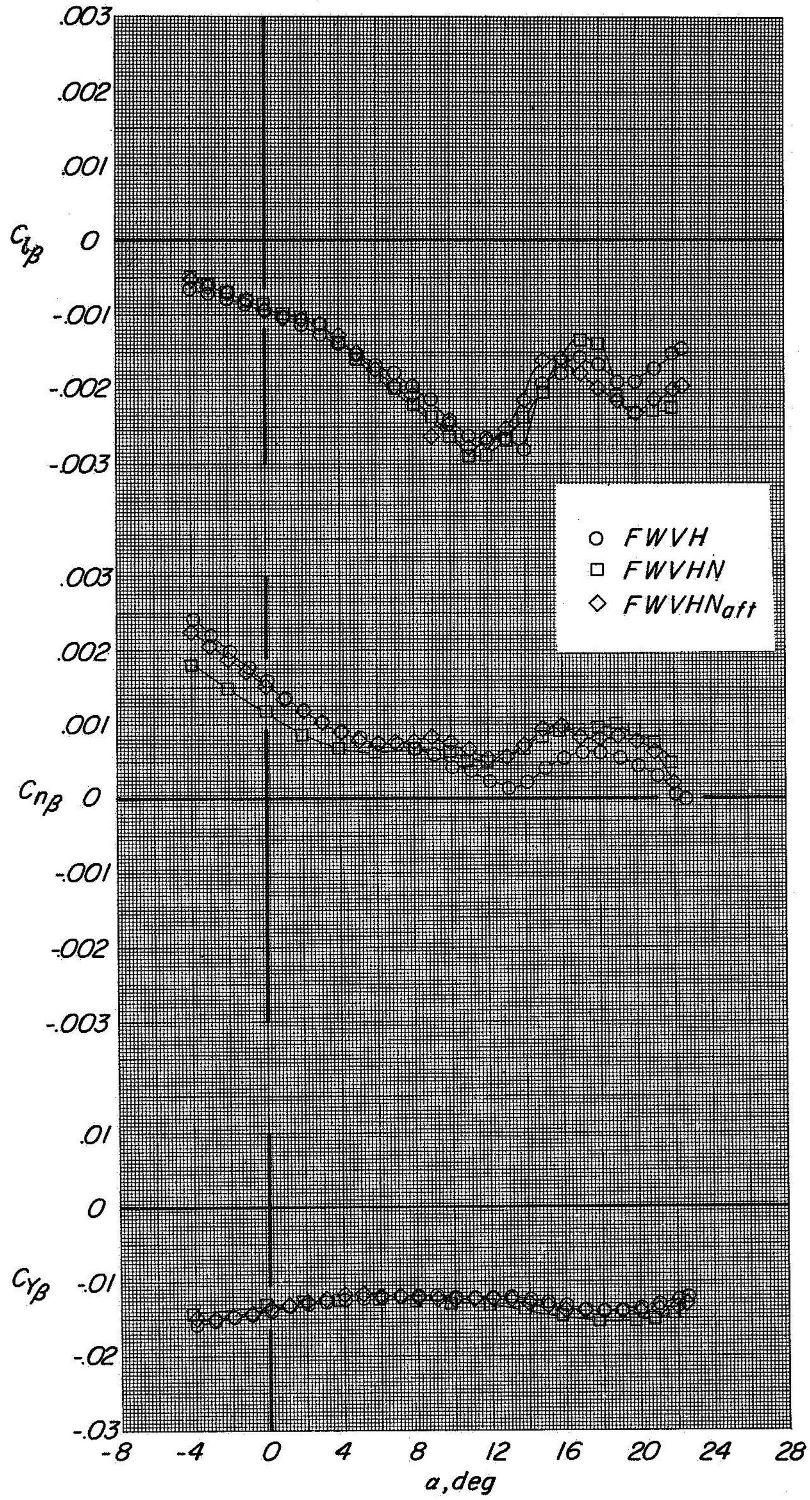

(b) Variation of C_{l_β}, C_{n_β}, and C_{Y_β} with α.

Figure 7.- Concluded.

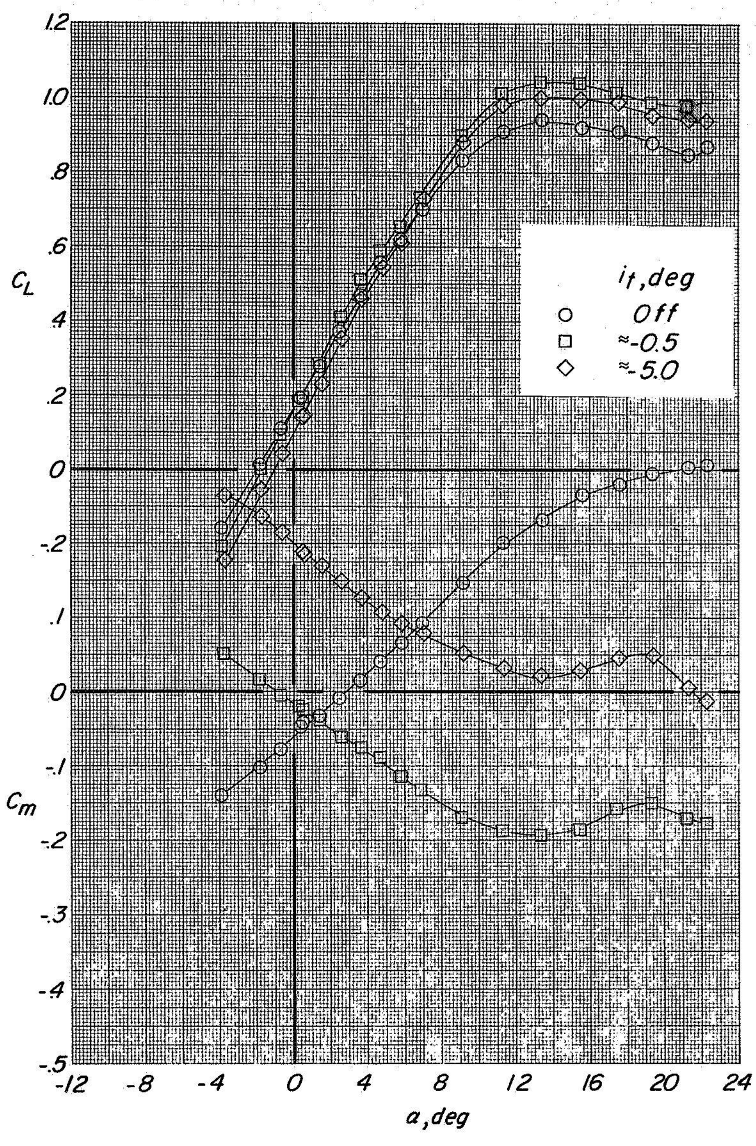

(a) Variation of C_L and C_m with α. $\beta = 0^0$.

Figure 8.- Lift, pitch, lateral, directional, and side-force characteristics of FWV with the horizontal tail off and on at various incidence angles.

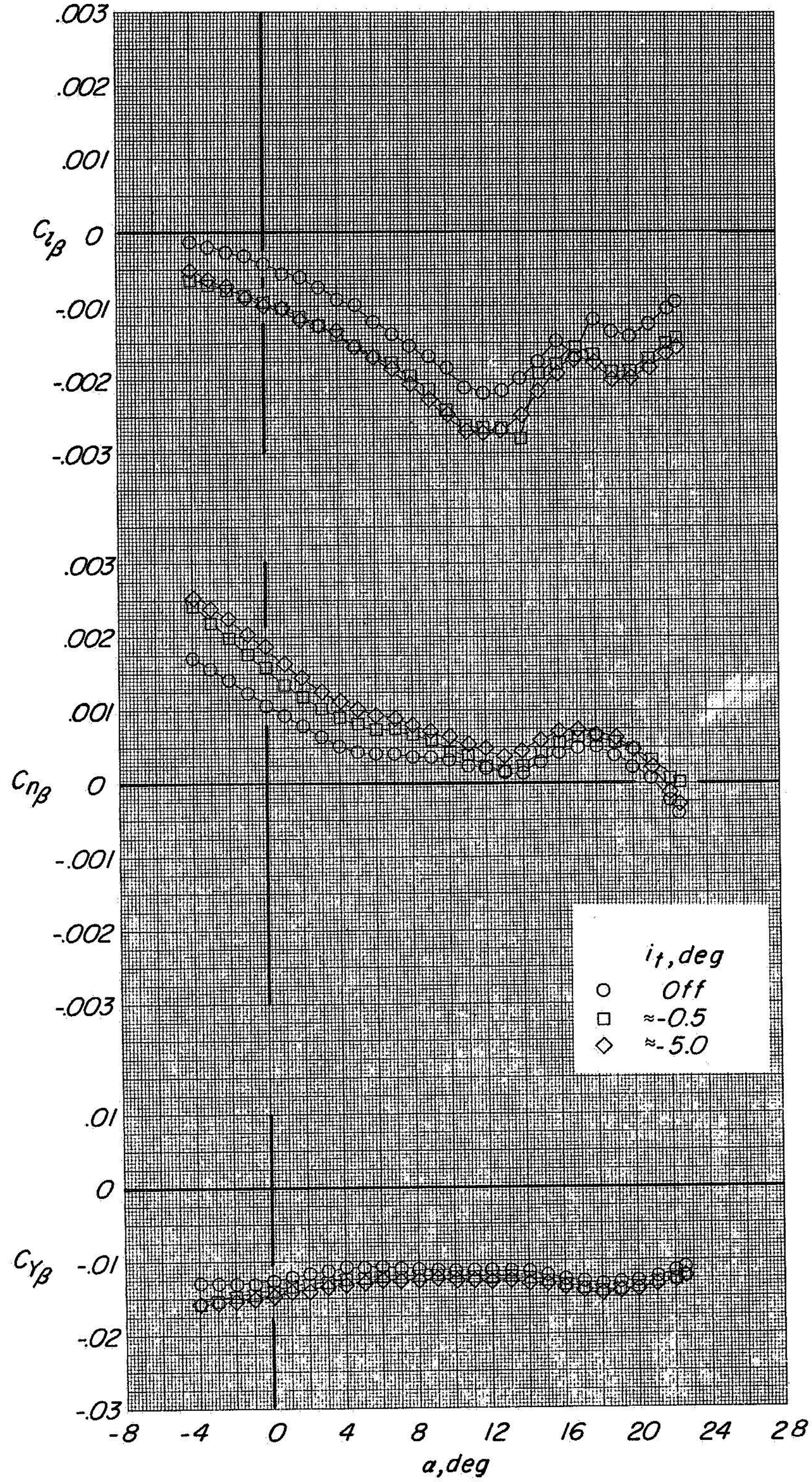

(b) Variation of C_{l_β}, C_{n_β}, and C_{Y_β} with α.

Figure 8.- Concluded.

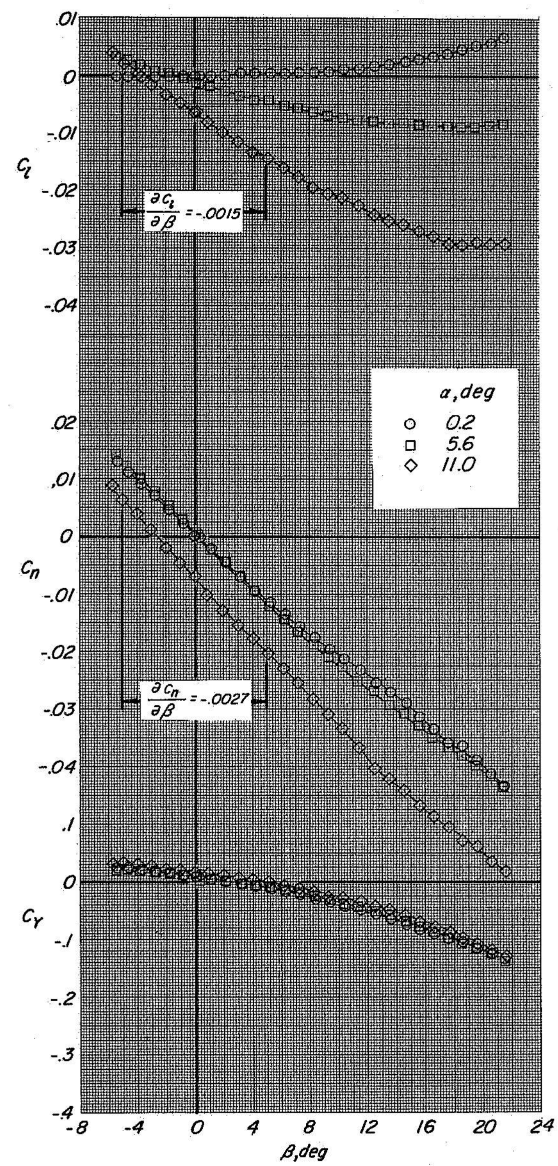

(a) FW.

Figure 9.- Effect of α on the variation of C_l, C_n, and C_Y with β.

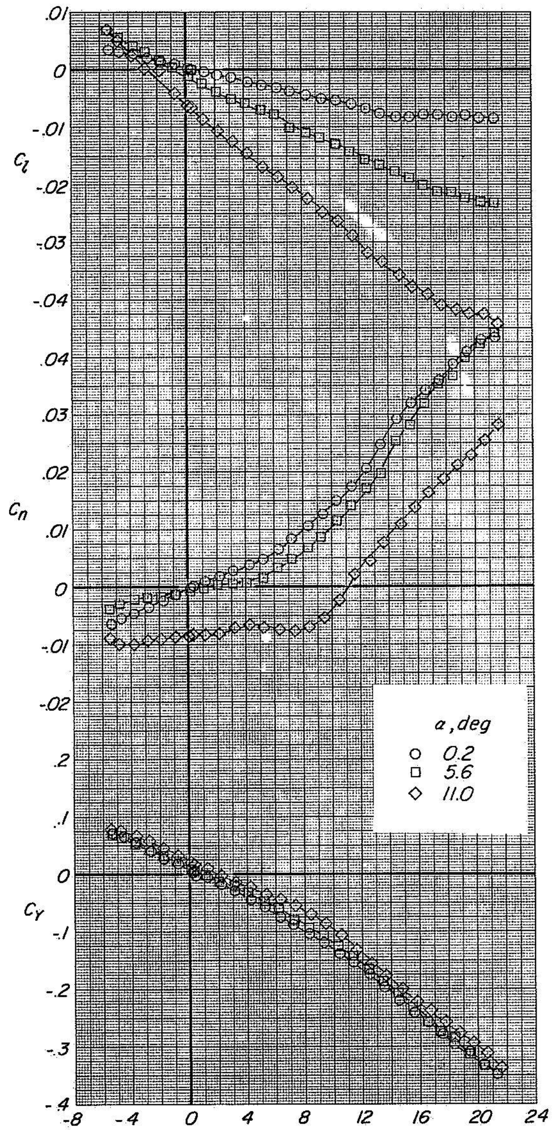

(b) FWV.

Figure 9.- Continued.

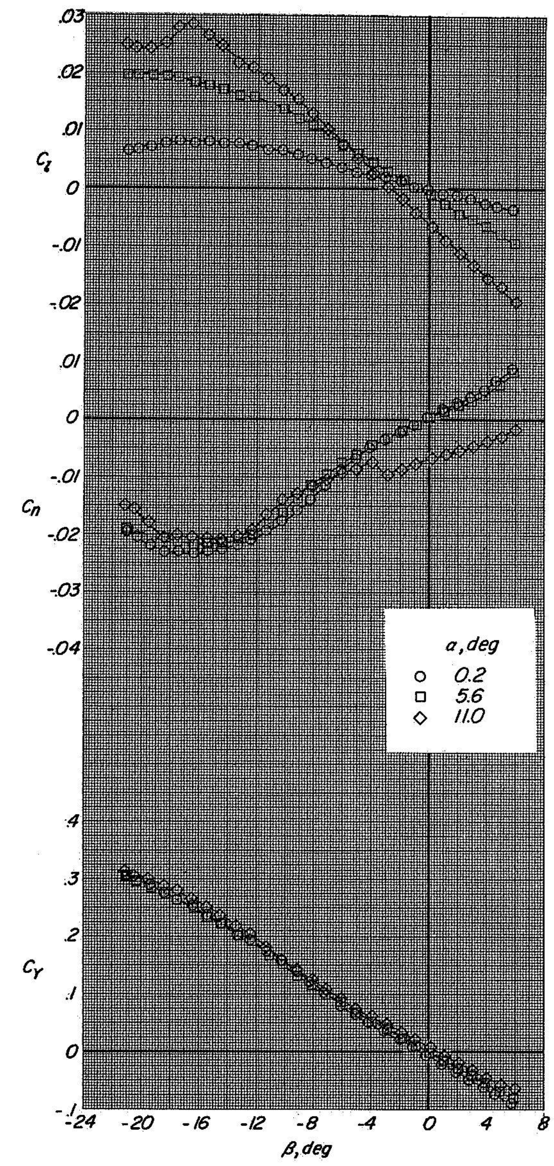

(c) FWV_1.

Figure 9.- Continued.

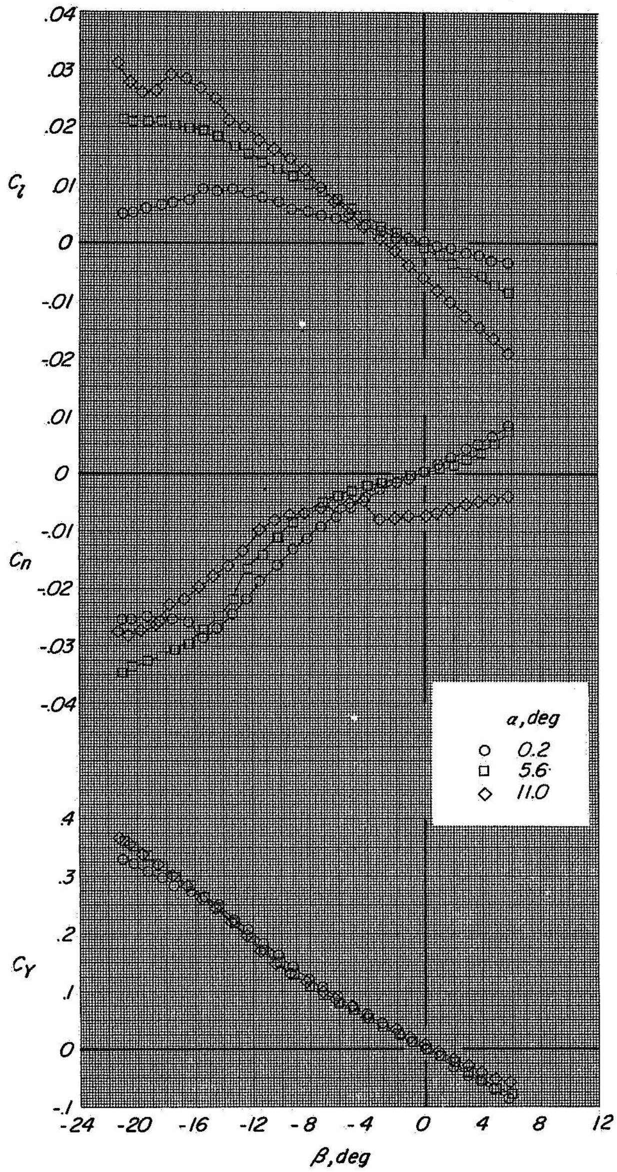

(d) FWV_2.

Figure 9.- Continued.

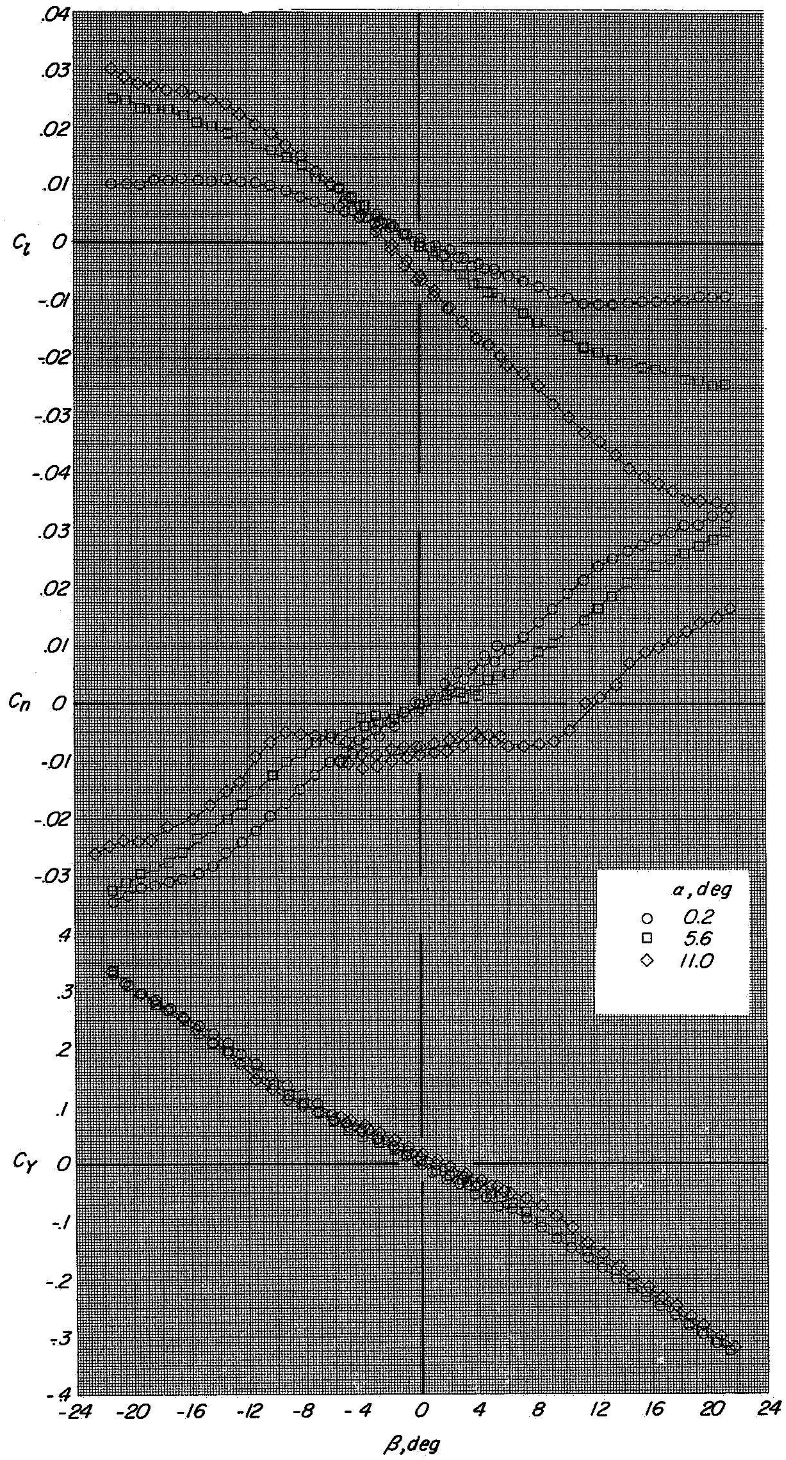

(e) FWVH ($i_t \approx 0^o$).

Figure 9.- Continued.

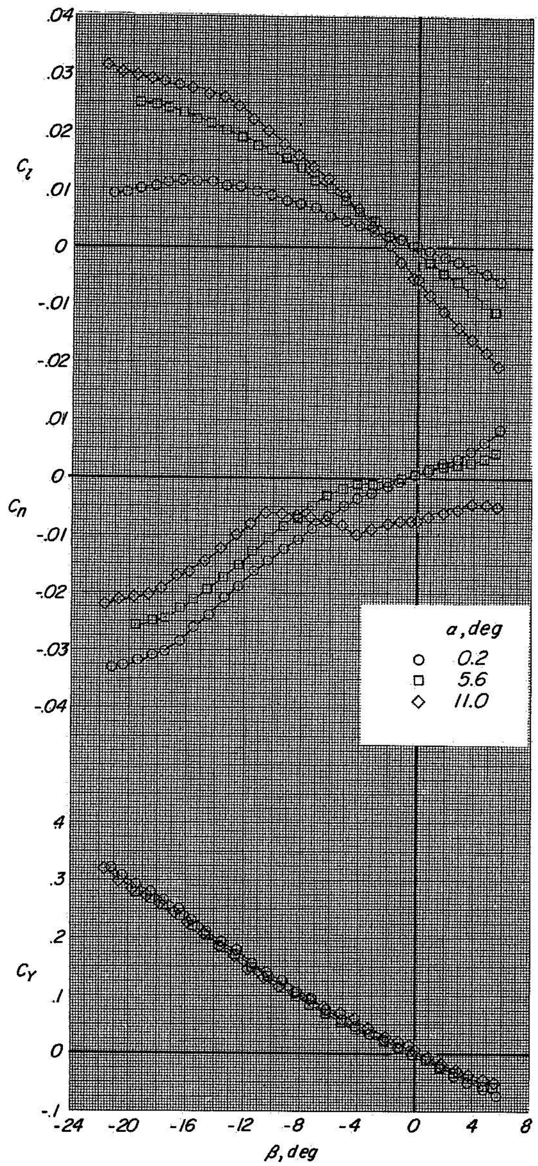

(f) FWVHN $\left(i_t \approx 0^0\right)$.

Figure 9.- Continued.

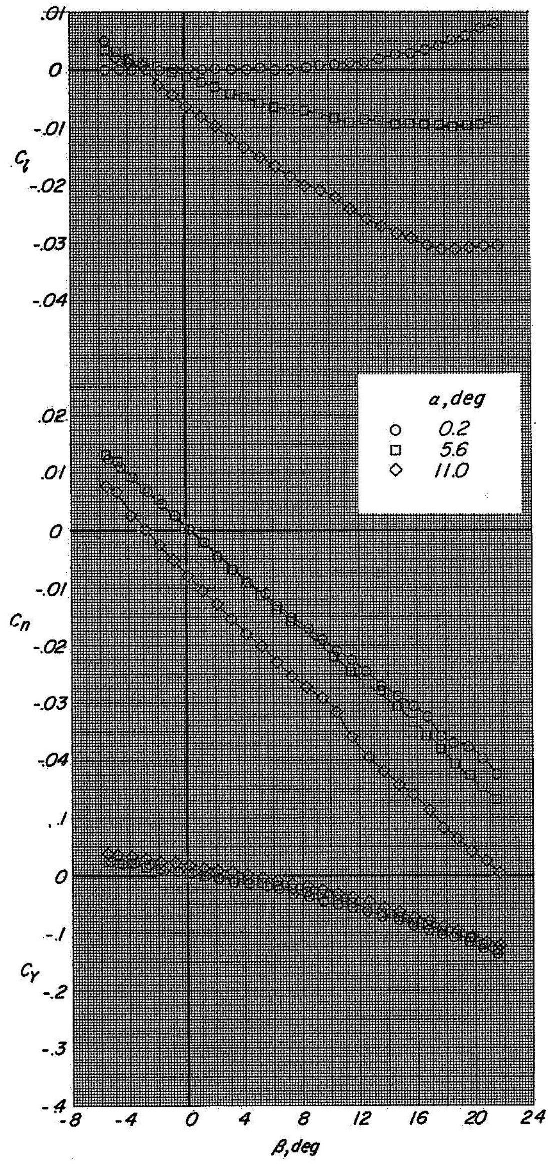

(g) FWN_{aft}.

Figure 9.- Continued.

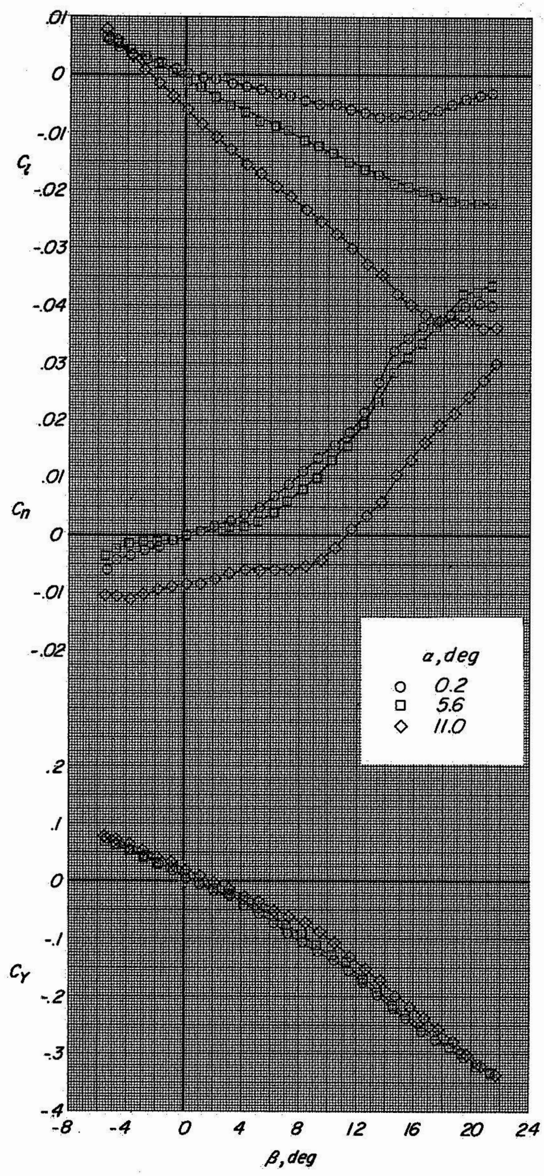

(h) $FWVN_{aft}$.

Figure 9.- Continued.

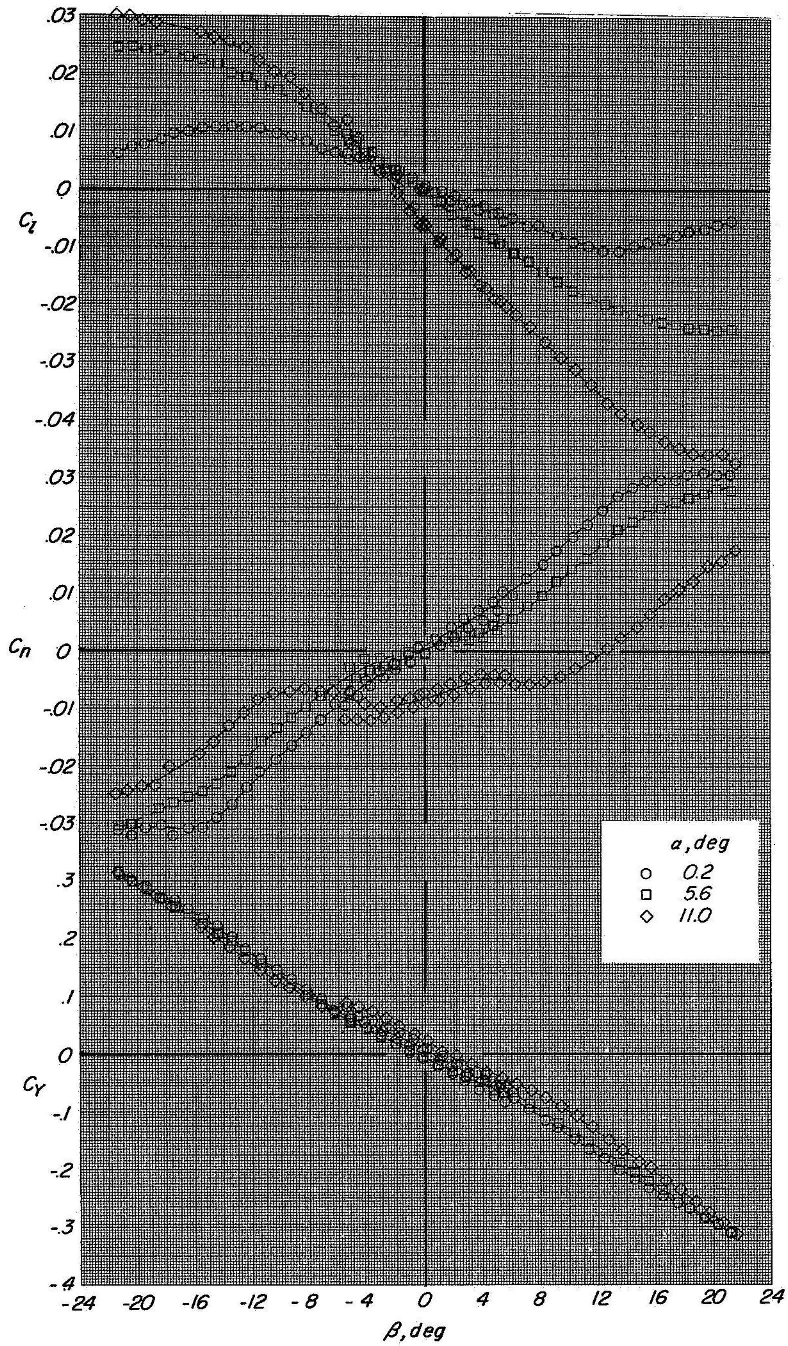

(i) $FWVHN_{aft}$ ($i_t \approx 0^0$).

Figure 9.- Continued.

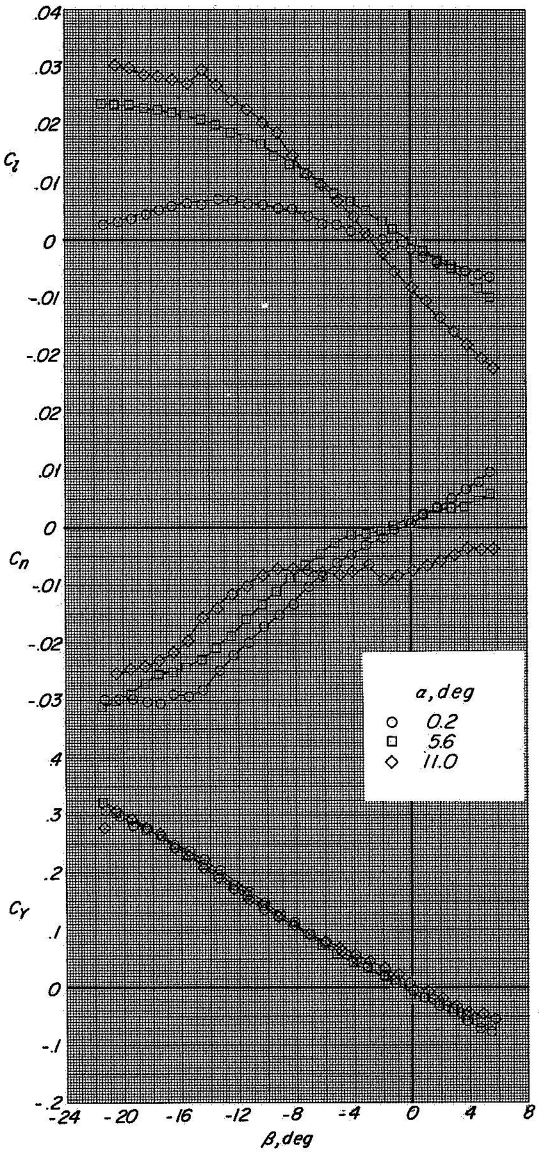

(j) $FW_fVHN_{aft}\left(i_t \approx 0^o\right)$.

Figure 9.- Concluded.

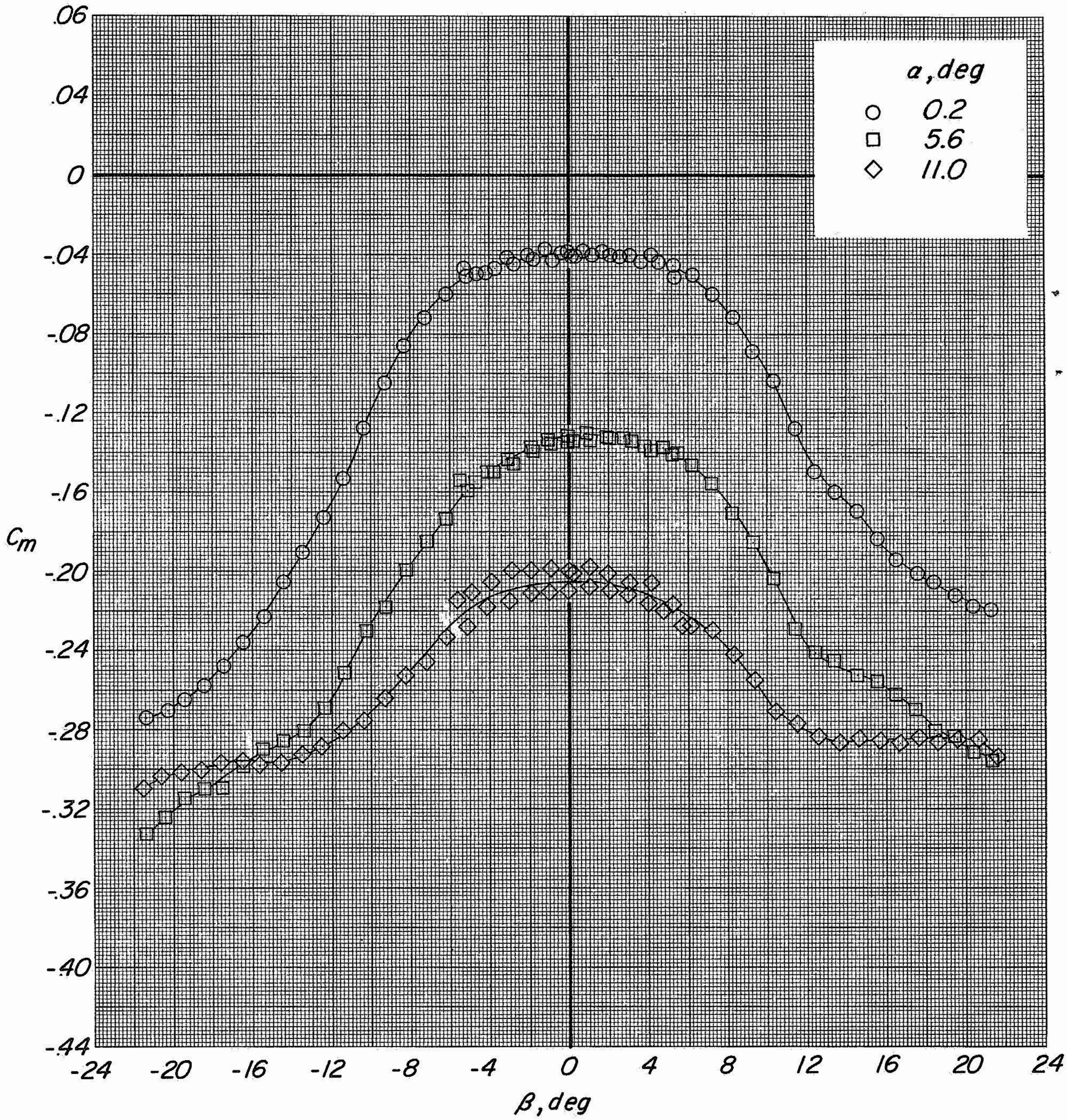

(a) FWVH $(i_t \approx 0^0)$.

Figure 10.- Variation of C_m with β at $\alpha = 0.2^0$, 5.6^0, and 11.0^0.

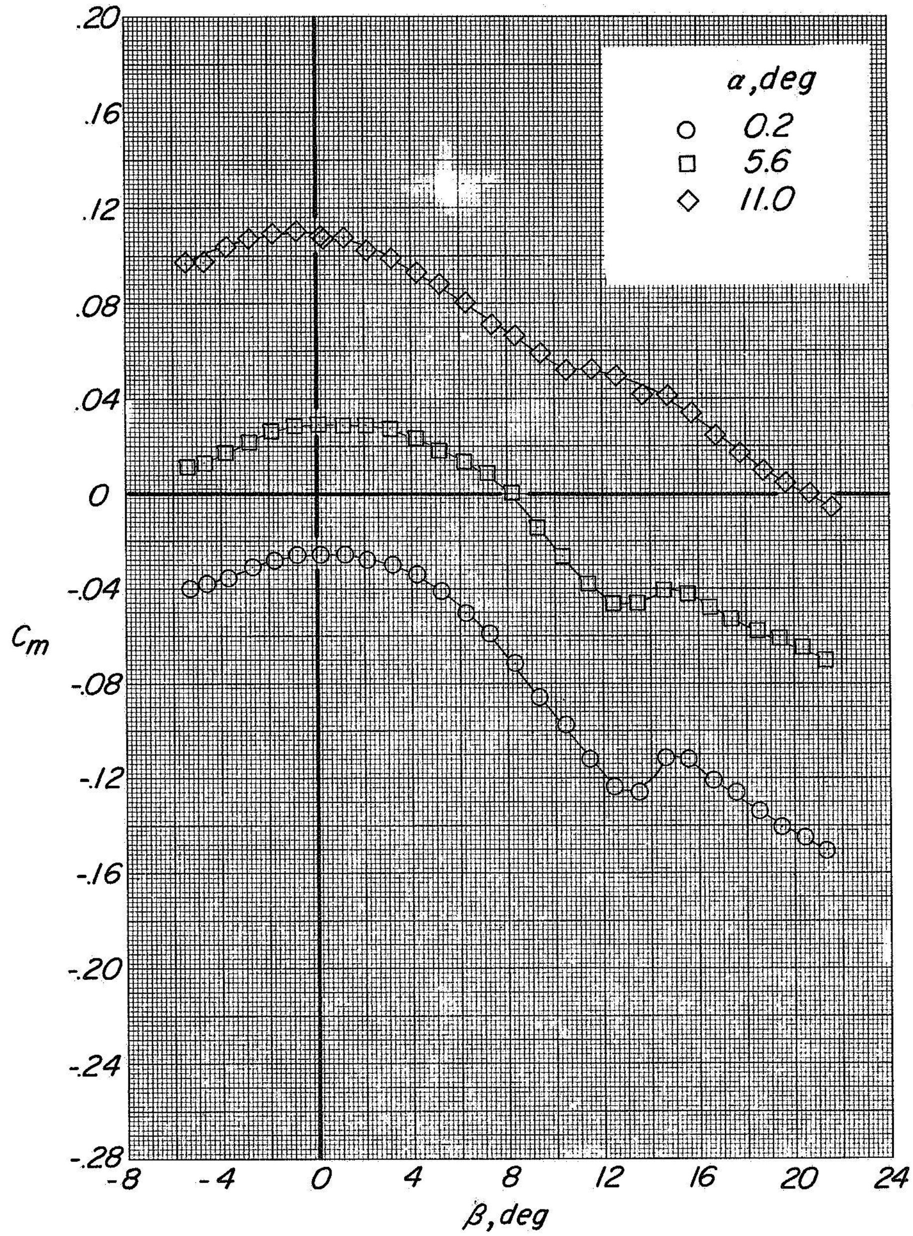

(b) $FWVN_{aft}$.

Figure 10.- Continued.

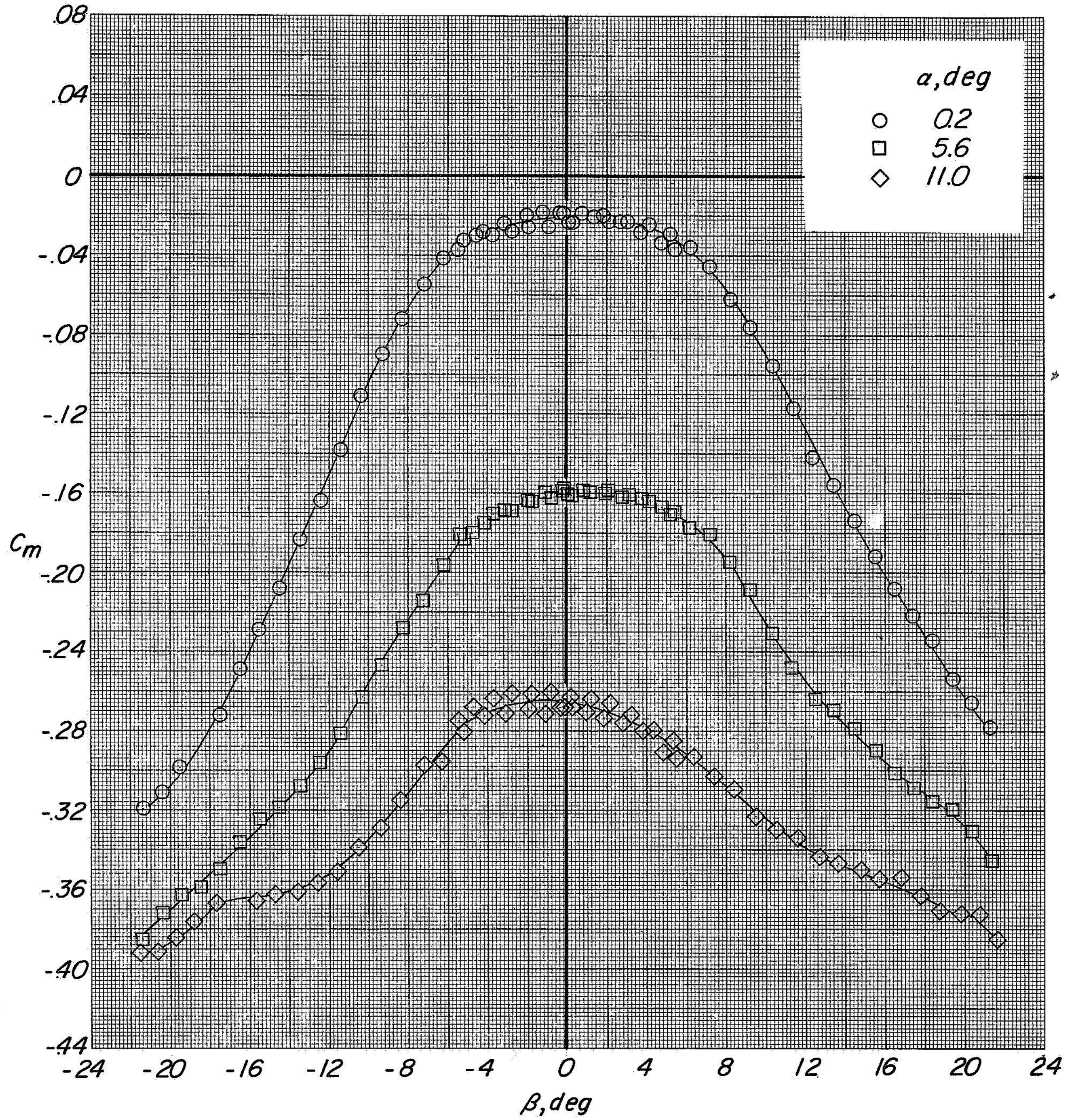

(c) $FWVHN_{aft}$ $\left(i_t \approx 0^{0}\right)$.

Figure 10.- Concluded.

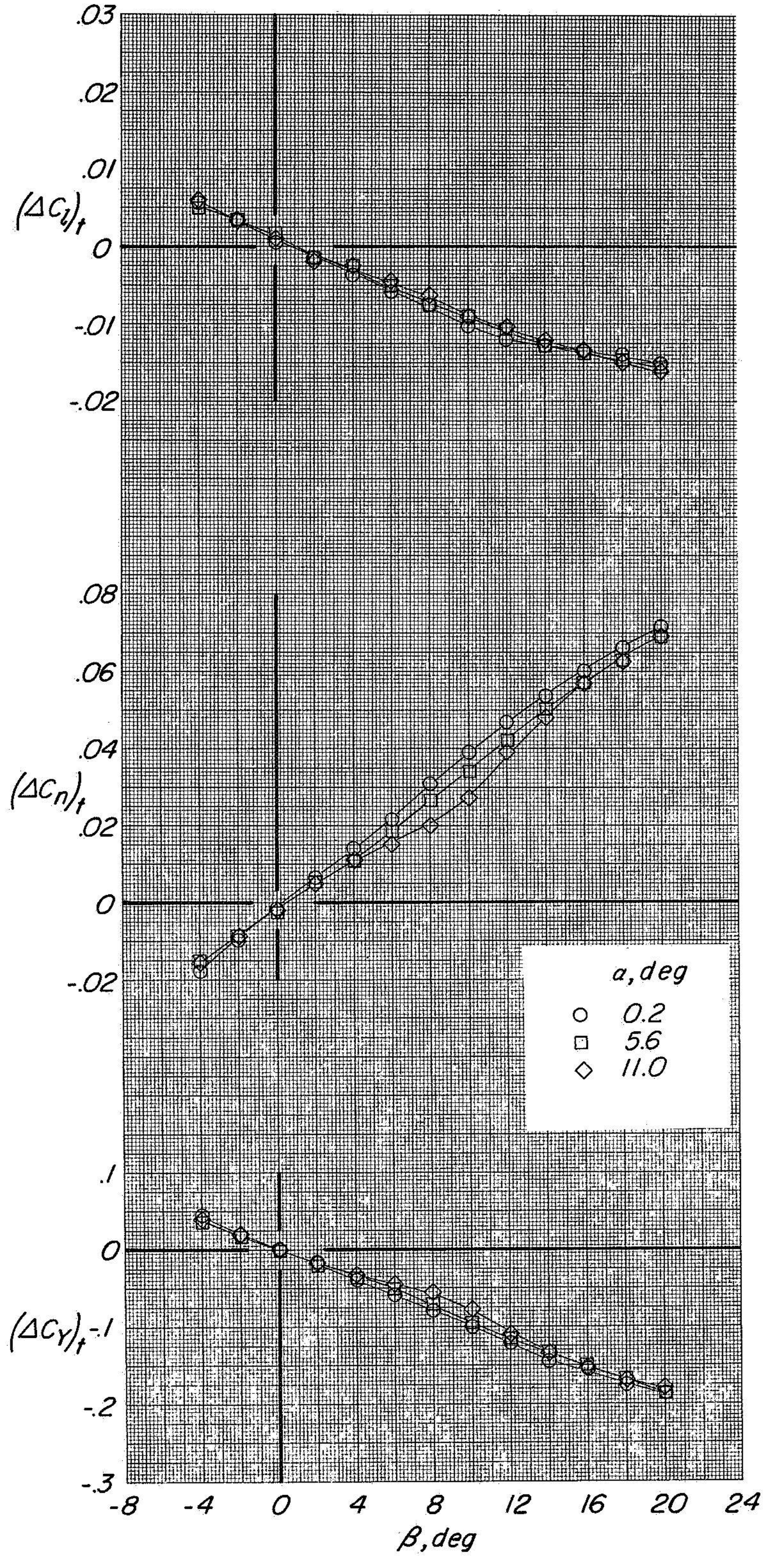

Figure 11.- Effect of combination of vertical and horizontal tails on sideslip characteristics of FW.

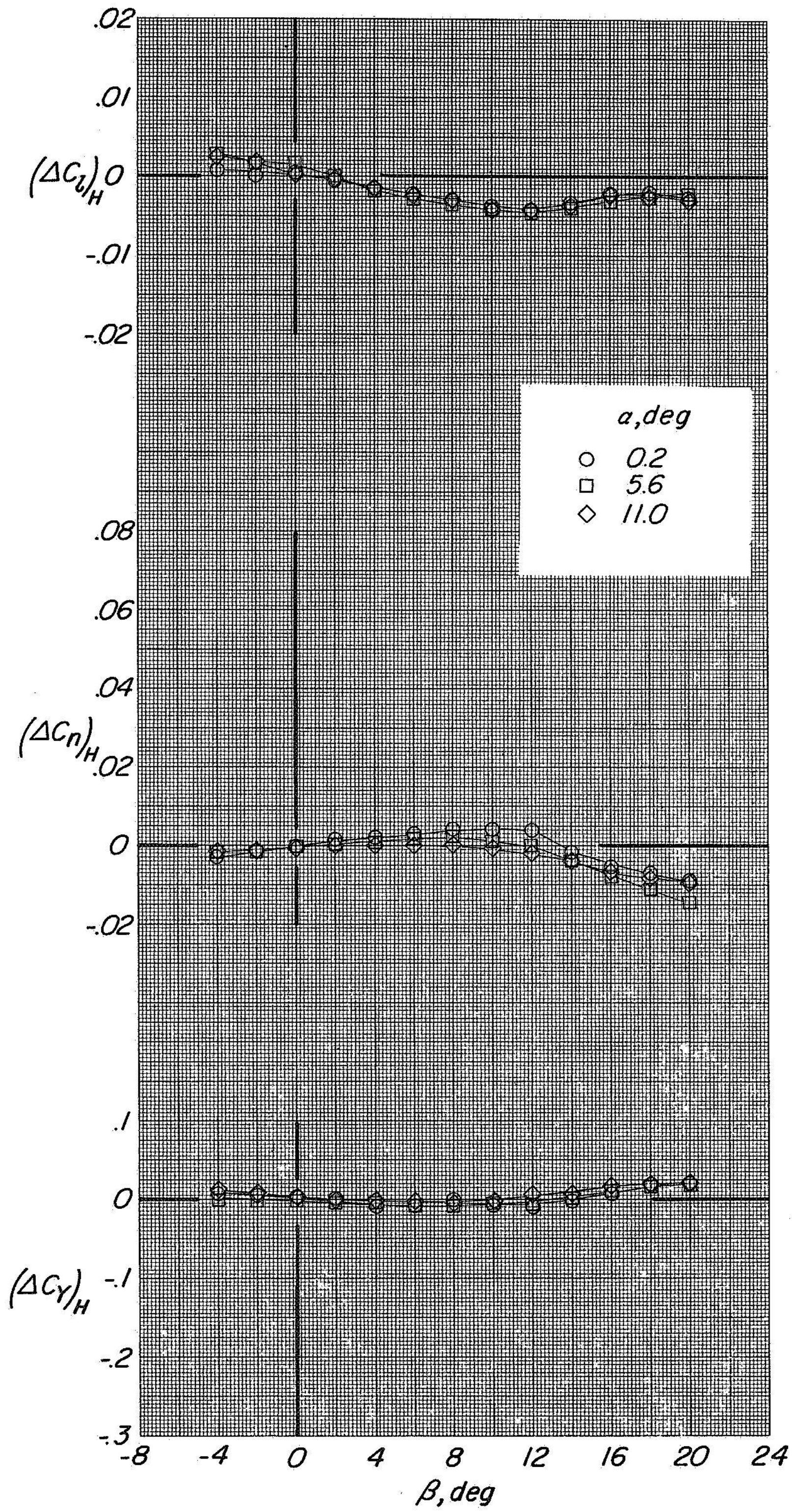

Figure 12.- Effect of horizontal tail on sideslip characteristics of $FWVN_{aft}$.

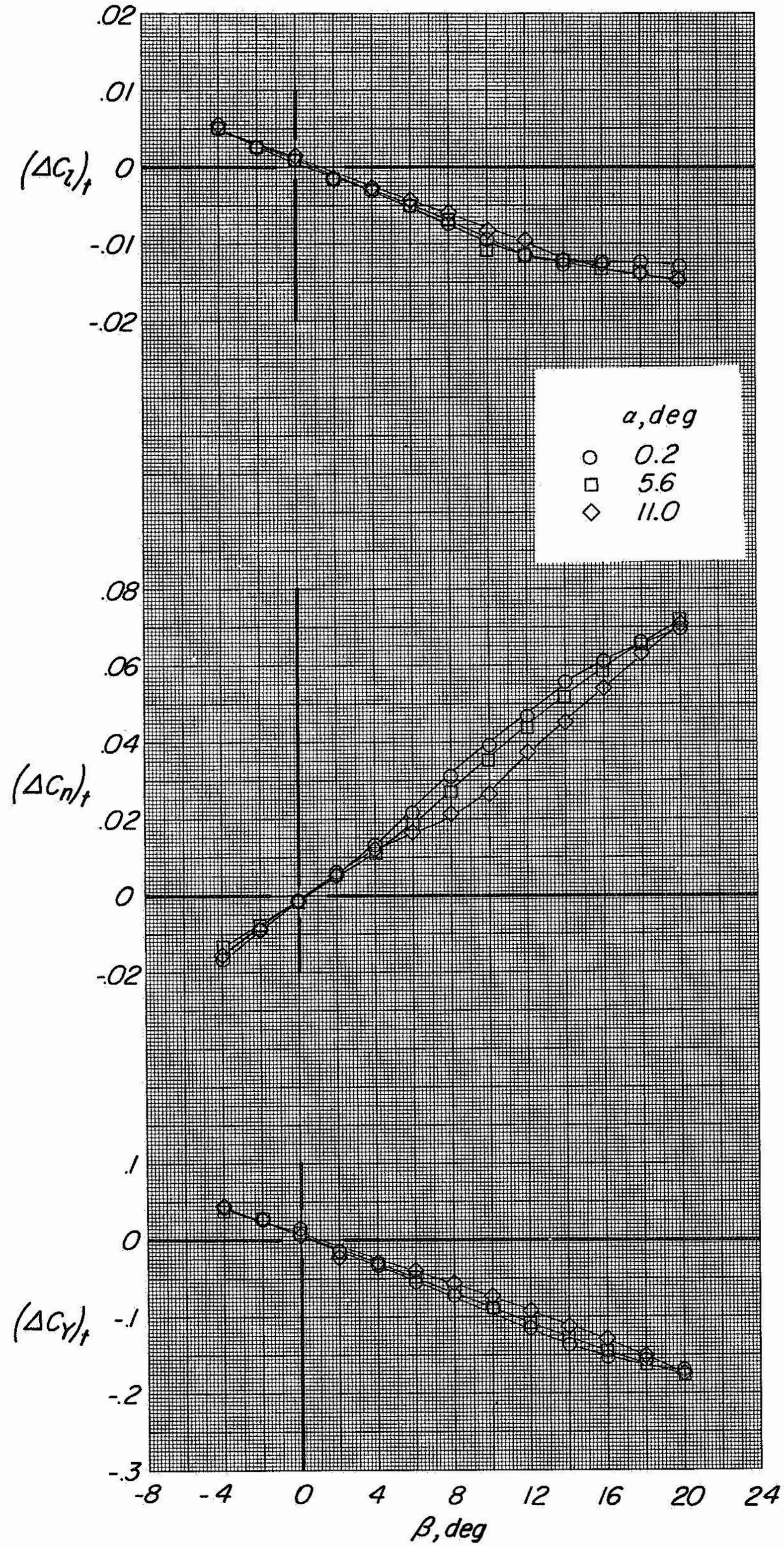

Figure 13.- Effect of combination of vertical and horizontal tails on sideslip characteristics of FWN_{aft}.

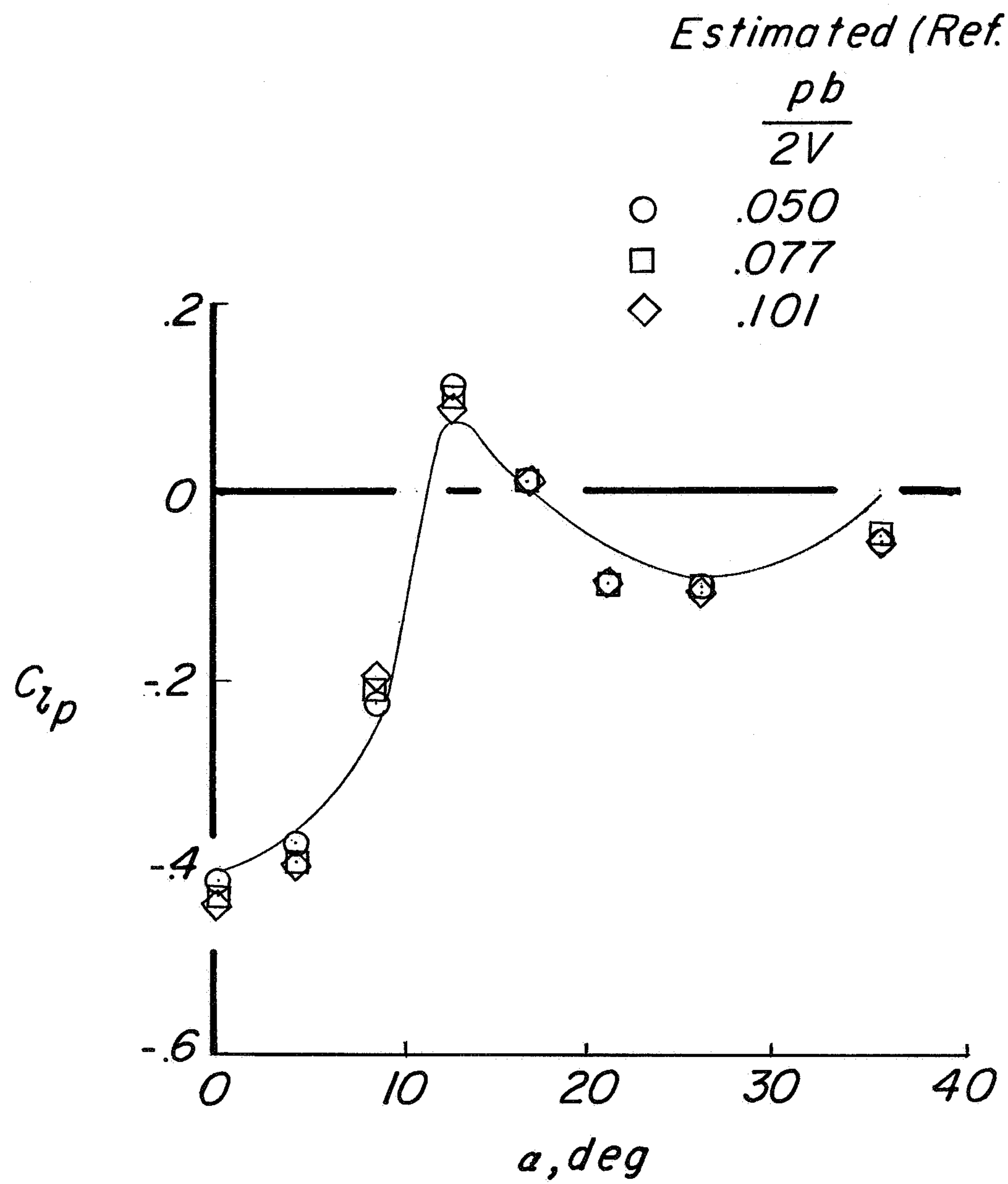

Figure 14.- Variation of C_{l_p} with α for FWVHN.

NASA-Langley, 1968 —— 1 L-6115

"The aeronautical and space activities of the United States shall be conducted so as to contribute . . . to the expansion of human knowledge of phenomena in the atmosphere and space. The Administration shall provide for the widest practicable and appropriate dissemination of information concerning its activities and the results thereof."

—NATIONAL AERONAUTICS AND SPACE ACT OF 1958

NASA SCIENTIFIC AND TECHNICAL PUBLICATIONS

TECHNICAL REPORTS: Scientific and technical information considered important, complete, and a lasting contribution to existing knowledge.

TECHNICAL NOTES: Information less broad in scope but nevertheless of importance as a contribution to existing knowledge.

TECHNICAL MEMORANDUMS: Information receiving limited distribution because of preliminary data, security classification, or other reasons.

CONTRACTOR REPORTS: Scientific and technical information generated under a NASA contract or grant and considered an important contribution to existing knowledge.

TECHNICAL TRANSLATIONS: Information published in a foreign language considered to merit NASA distribution in English.

SPECIAL PUBLICATIONS: Information derived from or of value to NASA activities. Publications include conference proceedings, monographs, data compilations, handbooks, sourcebooks, and special bibliographies.

TECHNOLOGY UTILIZATION PUBLICATIONS: Information on technology used by NASA that may be of particular interest in commercial and other non-aerospace applications. Publications include Tech Briefs, Technology Utilization Reports and Notes, and Technology Surveys.

Details on the availability of these publications may be obtained from:

SCIENTIFIC AND TECHNICAL INFORMATION DIVISION

NATIONAL AERONAUTICS AND SPACE ADMINISTRATION

Washington, D.C. 20546